ABSTRACT

Title of Document: EXPERIMENTAL EVALUATION OF A MULTIFUNTIONAL VARIABLE REFRIGERANT FLOW SYSTEM IN AN EDUCATIONAL OFFICE BUILDING

Laeun Kwon, Master of Science, 2013

Directed by: Dr. Yunho Hwang, Mechanical Engineering

The top three end uses - space heating, space cooling, and water heating – accounted for close to 41 percent of site energy consumption in U.S. building primary energy consumption. Therefore, energy efficient heating, ventilating and air-conditioning (HVAC) systems in buildings is essential for energy savings in the building sectors. A multifunctional variable refrigerant flow (MFVRF) system is finding its way into residential and commercial buildings since it can simultaneously provide space cooling, space heating and hot water.

The MFVRF system was installed in an educational office building and fully instrumented to measure the performance of the system under a wide range of outdoor weather conditions. The effects of a part-load ratio (PLR) on the daily performance factor (DPF) and total energy consumption were experimentally investigated in the field performance tests. Although the higher PLR represents a more effective cooling and/or heating the system, the DPF is not always increased with PLR because the system is optimized at a certain range of PLR. Furthermore, the

effects of the hot water demand and the heat recovery operation modes on the performance of the system were investigated in a field test for the heating and shoulder seasons.

Integrating the water heating functions into the heat recovery type variable refrigerant flow (HR-VRF) system, not only supplies hot water year-round, it also improves the system performance. As the hot water demand for the MFVRF system increased, the PLR was improved, which resulted in an increase system heating performance. In the heat recovery operation mode, the heat absorbed from the indoor units operating in the cooling mode was transferred to other indoor units operating in the heating mode. The DPF was 2.14 and 3.54 when the ratio of daily total cooling energy to daily total heating energy was 13.0% and 28.4%, respectively, at the similar outdoor weather conditions. This enhancement was attributed to the waste heat recovered during the heat recovery operation mode and the decrease in pressure ratio, which is a result of the improvement of the compressor efficiency.

Energy saving potential of the MFVRF system in a building with high internal heat gains, resulted in a high cooling load for the cooling season and a low heating load for the heating season, was verified through the field performance test. The performance of the MFVRF system for the heating and shoulder seasons was improved by transferring the recovered energy to the indoor space and supplying the hot water.

EXPERIMENTAL EVALUATION OF A MULTIFUNTIONAL VARIABLE REFRIGERANT

FLOW SYSTEM IN AN EDUCATIONAL OFFICE BUILDING

By

Laeun Kwon

Thesis submitted to the Faculty of the Graduated School of the

University of Maryland, College Park, in partial fulfillment

of the requirements for the degree of

Master of Science

2013

Advisory Committee:

Research Associate Professor Yunho Hwang (Chair)

Professor Reinhard Radermacher

Associate Professor Bao Yang

Dedication

to my parents and my fiancée, Hanah

Acknowledgements

I would like to acknowledge with deepest gratitude the contributions of my advisor, Dr. Yunho Hwang. He continually and convincingly conveyed a spirit of adventure in regard to research. Without his guidance and persistent help this work would not have been possible.

I am very grateful to my immediate supervisor, Dr. Radermacher, for his direction and help. I extend my appreciation to Jan Muehlbauer for his help and valuable ideas to my experimental work. I thank my colleagues for having been supportive, and made my time at CEEE much more enjoyable and unforgettable.

My thankfulness goes to those who supported this research: LG Electronics Inc. and CEEE at the University of Maryland.

Finally, I am thankful to my parents for encouraging me to pursue my graduate degrees. Last but not least, I would like to thank my fiancée, Hanah Park, for her support and understanding.

Table of Contents

List of Figures

List of Tables

1   Introduction

1.1   Background

In the United States, the buildings sector accounted for about 41 percent of primary energy consumption in 2010, 44 percent more than transportation sector and 36 percent more than the industrial sector [1]. Energy use in the building sector is divided into two categories: residential and commercial sectors. Of the total energy consumed in the building sector, the residential sector accounted for 54 percent and commercial buildings accounted for 46 percent.
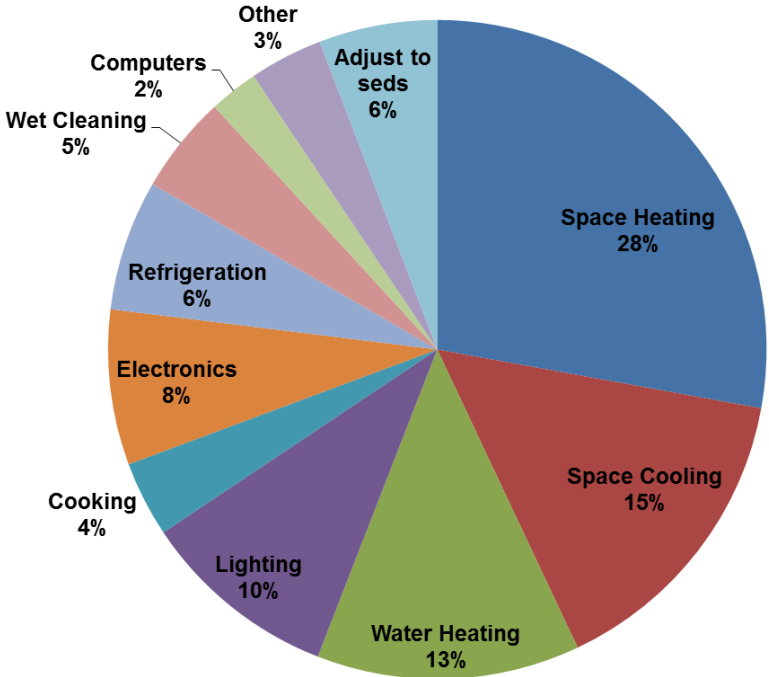
Figure 1.1: Residential site energy consumption by end use, 2010 [2]

Figure 1.1 shows the residential site energy consumption by end use in 2010. Most of energy was used in homes for space heating (28%), space cooling (15%), and water heating (13%) of the site energy consumption as shown in Figure 1.1.
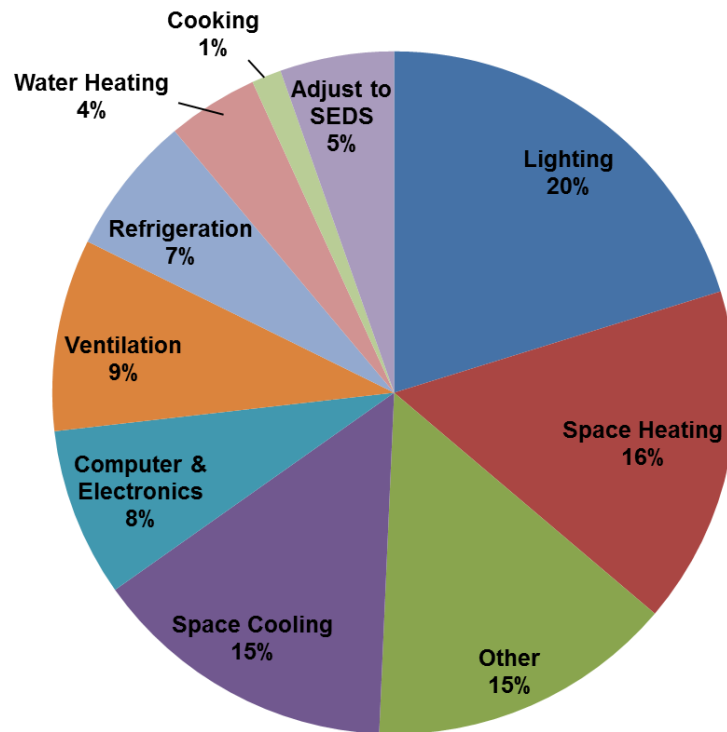
Figure 1.2: Energy use in commercial buildings, 2010 [3]

A commercial building includes offices, stores, restaurants, warehouses, hotel and other structures. Energy use in the commercial building is shown in Figure 1.2. The top three end uses in the commercial sector are space heating, lighting, and space cooling. These areas represent close to half of commercial site energy consumption. As shown in Figure 1.1 and Figure 1.2, most of the energy was used in residential and commercial buildings for space heating and cooling, and water heating. Therefore, the installation of the energy efficient heating, ventilating and air-conditioning (HVAC) systems in the building is essential for energy savings in the building sectors.

The most common types of the HVAC system are unitary air conditioners and heat pumps. Unitary air conditioners are factory-made assemblies that normally include an evaporator or

cooling coil and a compressor-condenser combination [4]. Heat pump system is capable of reversing the direction of refrigerant flow to provide either cooling or heating to the indoor space.

Unitary equipment is divided into three general categories: residential, light commercial, and large commercial. Residential equipment uses single-phase power with a cooling capacity of 19 kW or less and is designed specifically for residential application. Light commercial equipment generally uses three-phase power, with cooling capacity up to 40 kW, and is designed for small business and commercial properties. Commercial unitary equipment has cooling capacity higher than 40 kW and is designed for large commercial buildings [4].

For light and large commercial applications, HVAC options fall under one of three categories: packaged systems, split ductless systems, and variable refrigerant flow (VRF) systems [5]. The packaged systems include traditional boilers, chillers, water-source heat pumps and multi-zone rooftop units. Typically, conditioned air flows from the system to the indoor space through ductwork. Split systems have two parts, usually an indoor air-handling unit and outdoor unit housing the compressor. Again, the components of this system can include boilers, chillers and water source heat pumps, etc. A split ductless system is comprised of a remote outdoor condensing unit connected by refrigerant pipes to a matching, non-ducted indoor air handler. In some special cases, a limited ducting is used from outside to the air handler for introducing fresh air. Finally, the VRF systems are a flexible variety of a more traditional option. The key difference is that VRF system responds to changes in cooling and heating requirements by varying the refrigerant flow to individual zones - as opposed to moving cooled or heated air through ductwork to those spaces.

VRF systems are now the preferred HVAC system for small and medium commercial buildings and large residential applications, such as high-rise apartment and multi-family buildings in both Asia and Europe. It is estimated that VRF systems serve for more than 50 percent of Japanese commercial buildings with less than 70,000 square feet, and 15 percent of larger buildings [6]. VRF systems were introduced in the U.S. at around 2002, and have been installed in many types of commercial buildings, including offices, hotels, luxury apartments, low-income multi-family buildings and universities [6].

1.2 VRF System

VRF systems are very similar to traditional heat pump systems, but they use inverter drives for compressors to vary their capacity, similar to mini-split (ductless) heat pumps. VRF systems have many significant advantages, such as integrated controls, quiet operation, design and installation flexibility, compact equipment, lowered lifecycle cost and reduced maintenance cost. Also, VRF systems do not experience the same energy losses as systems that distribute the conditioned air through ductwork. There are two basic types of VRF systems: cooling and heating only systems, and simultaneous cooling and heating systems. The former is called as "heat pump type VRF (HP-VRF)" system, the latter is "heat recovery type VRF (HR-VRF)" system.

1.2.1 Heat Pump Type VRF System

HP-VRF system operates in either heating or cooling mode at any given time. In HP-VRF system, all indoor units are operated in same mode. They have a wide range of indoor units, from floor standing units to concealed ducted units. There would usually be only one outdoor unit

4

(depending on the size/duty of the design) with interconnecting pipework in one main run between outdoor unit and indoor units.
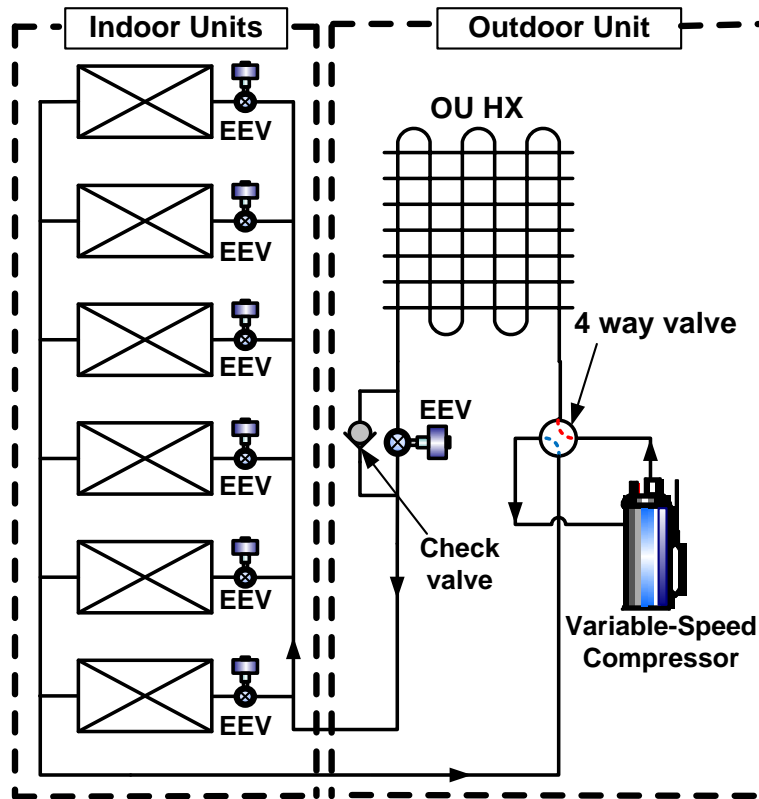
Figure 1.3: Schematic diagram of the heat pump type VRF system

Figure 1.3 shows the schematic diagram of the HP-VRF system which is equipped with six indoor units and one outdoor unit (OU). OU consists of a variable-speed compressor, a four-way valve, a fan, a heat exchanger and an electronic expansion valve (EEV). Each indoor unit (IU) has a heat exchanger, fan and EEV. It is very similar to traditional heat pump systems. All IUs connected to the OU have the ability for individual control and achieving set point thanks to the inverter driven compressor and EEVs.

In the cooling mode of the HP-VRF system, the high pressure and temperature gas refrigerant discharged from the compressor flows into the outdoor unit heat exchanger. Phase change process occurs at the outdoor unit heat exchanger from gas to liquid after rejecting heat to the ambient. High pressure and medium temperature liquid refrigerant from the OU heat exchanger passes through the EEV of each indoor unit. Through the expansion process at the EEV of each indoor unit, temperature and pressure of the refrigerant are dropped and undergo evaporation process with the circulating air from the indoor space. In the heating mode, the refrigerant flow direction is reversed by the four-way valve. High pressure and temperature gas refrigerant flows into the indoor units and then back to the outdoor unit. Before entering the OU heat exchanger, expansion process occurs at the main EEV in OU. Then, the refrigerant flows back to the compressor after it has absorbed heat from the ambient.

1.2.2   Heat Recovery Type VRF System

The second type of VRF is a HR-VRF system that can provide heating and cooling at the same time. To match building's load profiles, heat is transferred from one indoor space to another through the refrigerant line. Such recovery operation is necessary when there is a need to switch modes between cooling and heating for day and night, during the shoulder season, or when there is a difference in room temperatures due to the influence of solar radiation in zones. It is also necessary when there is a need to cool offices year-round – arising from the widespread use of computers and terminal devices.

Recently, the heat generated inside buildings is less likely to be released to outside building due to changes in building structures, such as the improvement of thermal insulation performance

and the use of multi-pane windows. Cooling is required throughout the year in the interior zone where there is a great deal of lighting fixtures and office equipment. Meanwhile, in the perimeter zone (which is easily affected by ambient temperature and solar radiation), either cooling or heating is required depending on changes in heat balances.

Applications of the HR-VRF system are office buildings, hospitals, schools and multi-family building. HR-VRF systems can also provide hot and cold water from the same system. For most commercial and industrial applications this would be a great way to reduce energy cost, as heat removed from the building could be utilized for producing hot water in the cooling season. Figure 1.4 shows the schematic drawing of the HR-VRF system. It consists of an OU, a heat recovery unit (HRU), and four indoor units. The components of the outdoor unit and indoor units are same as those of the HP-VRF system. All IUs, connected to a HRU, not only have the ability for individual room temperature control, but they can also be individually operated in either heating or cooling mode any time. A HUR consists of header pipes, branch pipes, and solenoid valves. The solenoid valves control the refrigerant flow path entering into each IU, which changed the operation mode of IU. There are three pipes between OU and HRU. The three pipes between the OU and HRU are classified according to the refrigerant phase, high pressure and temperature gas pipe, high pressure and medium temperature liquid pipe, and low pressure and temperature gas pie. Each indoor unit is connected to the HRU with two pipes, gas and liquid pipes.
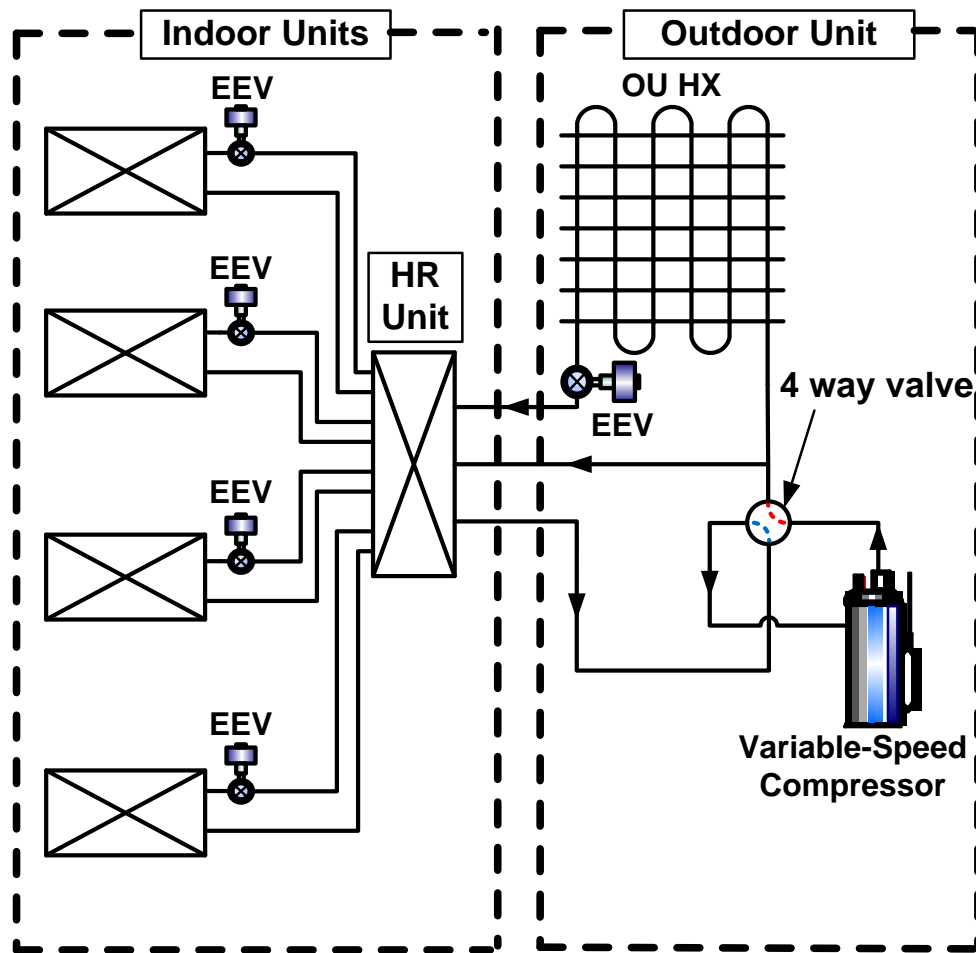
Figure 1.4: Schematic drawing of the heat recovery type VRF system

HR-VRF system can be operated in five operation modes: heating-only, cooling-only, heating-based operation, cooling-based operation and cooling-heating operation mode. Cooling-only and heating-only operations are same as the cooling and heating operation mode of the HP-VRF system, respectively. Heat recovery operation means when a HR-VRF system is operated in one of following modes: the cooling-based operation, heating-based operation or cooling-heating operation mode.

As an example of the heat recovery operation modes, refrigerant flow paths in the cooling-based operation mode are shown in Figure 1.5. Refrigerant flow discharged from the compressor splits into two paths at the location A: the one passes through the outdoor unit heat exchanger and the other bypasses and goes to the HRU. The bypassing high pressure and temperature gas refrigerant flows through the heating-operated indoor units, then it merges into the header pipe, which is represented as yellow color in the HRU (where the refrigerant from the outdoor unit heat exchanger is mixed).

The high pressure and medium temperature liquid refrigerant in the header pipe of the HRU flows through the indoor units operating in the cooling mode. The refrigerant flow direction is controlled by four-way valves and solenoid valves. An outdoor heat exchanger is used as a condenser in the cooling-only and cooling based operation mode, and as an evaporator in the heating-only and heating based operation mode.
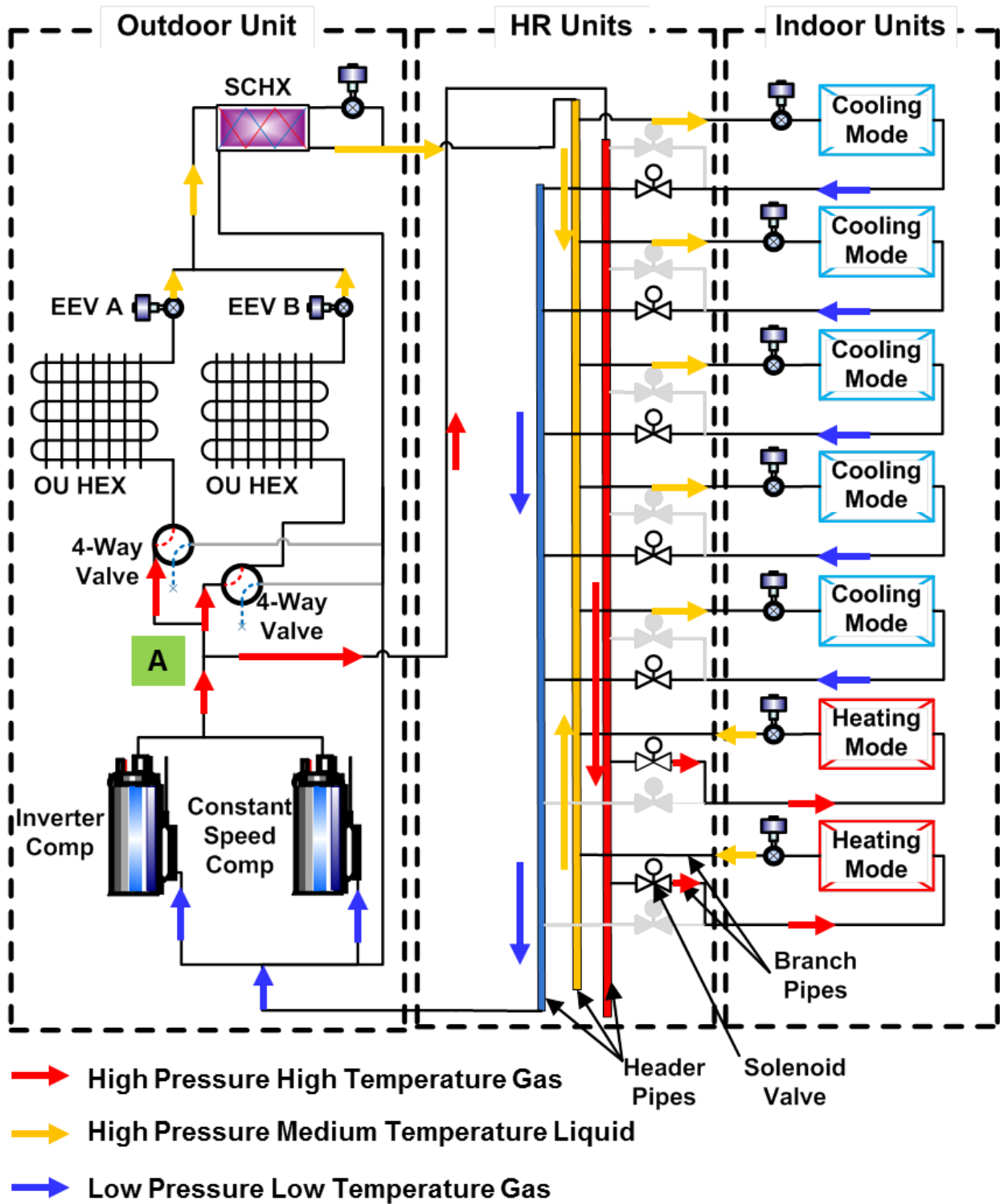
Figure 1.5: Refrigerant flow paths of HR-VRF system in cooling based operation mode

1.3   Heat Pump Water Heater

Heat pump water heaters use electricity to absorb heat from ambient air to heat water. Therefore, they are two- to three-times more energy efficient than conventional electric resistance water heaters [7]. Most homeowners who have heat pumps use them to heat and cool their homes. However, a heat pump also can be used to heat water, either as a stand-alone water heating system or as a combined water heating and space conditioning system. Figure 1.6 shows a diagram of a stand-alone heat pump water heating system. The condenser is immersed in the water tank to heat water.
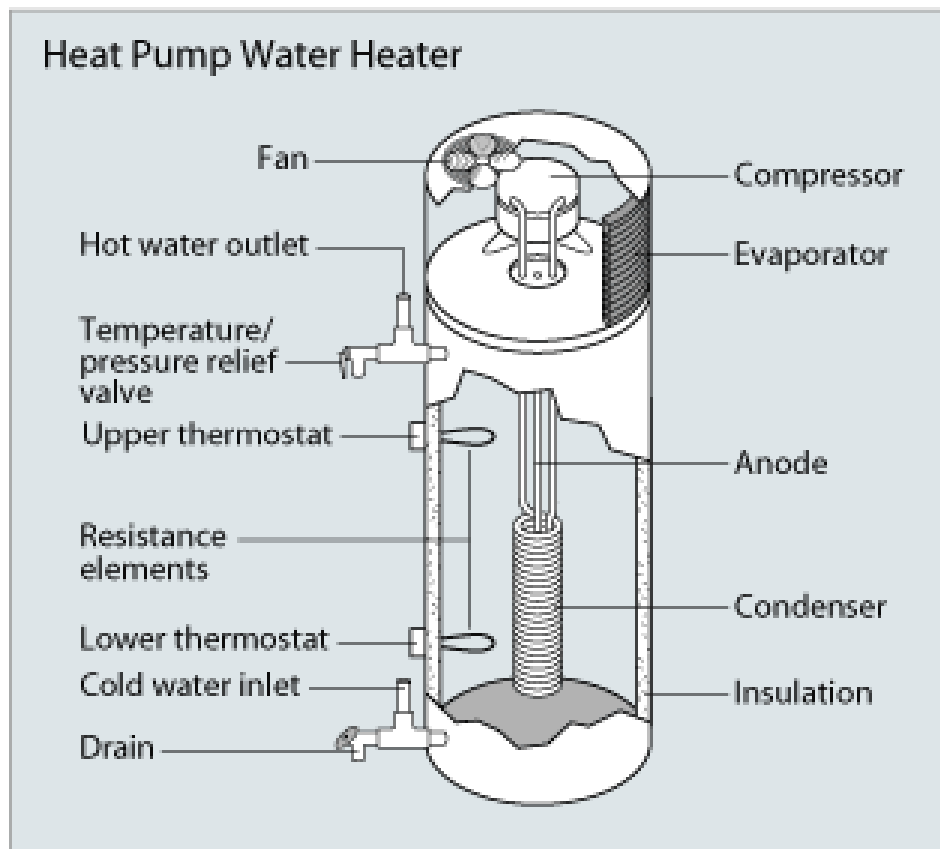
Figure 1.6: A diagram of a stand-alone heat pump water heating system [7]

11

In the heat pump system, the waste heat from the condenser can be utilized to produce hot water during the cooling mode. One major shortcoming of the combined water heating and space conditioning system is that hot water is not always available, since the condensing waste heat is only available while the system is operated in cooling mode.

2   Literature Review

2.1   HP- and HR-VRF Systems

Many researches on HP-VRF system were performed theoretically and experimentally. Park et al. [8] theoretically analyzed the performance of the air conditioner with two evaporators and EEVs. The effects of the compressor operating frequency, the loads of the conditioned rooms and the opening area of the EEVs on the performance of the system were investigated. They reported that total capacity of the system was mainly controlled by the compressor operating frequency. Furthermore, the EEV opening controlled the refrigerant mass flow rate through the evaporators. Fujimoto et al. [9] evaluated the performance of VRF air-conditioning system with three different methods of measuring the refrigerant flow rate, using an ultrasonic volume flow meter, a Coriolis flow meter, and a compressor performance map.

Its performance, measured based upon the refrigerant enthalpy method, was compared with the performance measured by the air enthalpy method. This showed that the refrigerant enthalpy method using a Coriolis flow meter is effective under a wider range of conditions than using an ultrasonic volume flow meter. Hu and Yang [10] applied the variable capacity scroll type compressor to the multi-type air conditioner without using inverter technology. They found that the developed system could adjust the capacity within 17 - 100% with a power input of 1.3 - 4.8

kW, on the other hand, the inverter system adjusted the capacity within 48 - 104% with a power input of 2.5 - 6.1 kW. Zhang et al. [11] evaluated the performance of the HP-VRF system under part load conditions. Hourly heating performance factor and hourly heating energy efficiency ratio were analyzed by the experimental test results. When the part-load ratio (PLR) was in the range of $0.7 - 0.9$, hourly heating energy efficiency ratio was higher than that of the other PLR range. Kwon et al. [12] investigated the effect of a subcooling heat exchanger (SCHX) on a HP-VRF system in a field test during the cooling season. It was concluded that the HP-VRF system equipped with SCHX improved the cooling performance factor (CPF) about 8.5%, as compared to the baseline without a SCHX.

Building energy simulation programs, such as EnergyPlus, EnergyPro and eQUEST, are used to evaluate the performance of the HVAC system in a building. Zhou et al. [13] developed the HP-VRF simulation module in the EnergyPlus and then validated against experimental data. It was found that the mean relative error was 28.31% for the VRV system power use simulation while 25.19% for the system cooling energy simulation. Li et al. [14] developed the simulation module for the HP-VRF system with water-cooled condenser in EnergyPlus program. After modeling and testing the developed module, simulation comparison was performed with the fan-coil plus fresh air (FPFA) system, and air-cooled HP-VRF system. It was found that, during the whole cooling period, the FPFA system consumed about 20% more power than the water-cooled HP-VRF system. The water-cooled HP-VRF system consumed only about 4% more power than the air-cooled one. Kwon et al. [15] validated the result obtained from the building energy simulation program, EnergyPlus, against the field performance test result of HP-VRF system. It was found that the mean of the absolute values of the daily, weekly and monthly relative error

were 6.8%, 2.4% and 2.2%, respectively. Aynur et al. [16] numerically compared the two widely used air conditioning systems, variable air volume (VAV) and HP-VRF system, in an existing building for an entire cooling season. The energy-saving potentials of the HP-VRF system were expected to be 27.1%-57.9%, as compared with the VAV system.

Since the main drawback of the VRF system is its inability to provide the ventilation, the VRF system in conjunction with a ventilation system was studied [17, 18]. Aynur et al. [17] performed a field test to investigate the effects of the ventilation and the control mode on the performance of the HP-VRF system integrated with a heat recovery ventilation (HRV) in both cooling and heating seasons in an office suite. It was found that the HP-VRF system in the individual control mode provided better thermal comfort than the HP-VRF system in the master control mode in both cooling and heating seasons. Also, due to the additional ventilation load, the ventilation combined HP-VRF system consumed higher energy than the non-ventilated system. The VRF system equipped with an additional ventilation system, such as heat recovery ventilation unit and a self-regenerating heat pump desiccant unit was introduced and experimentally investigated in a field performance test by the Aynur et al. [18]. It was found that the HP-VRF system consumed 26.3% less energy when it was operated with the heat pump desiccant unit as compared to the operation with the HRV unit.

Although many researches on HP-VRF systems have been performed as summarized above, studies on HR-VRF system are limited in open literature. Joo et al. [19] investigated the performance characteristics of a simultaneous cooling and heating multi-heat pump system under partial load conditions in a psychrometric chamber. It was concluded that the COP of the HR-

VRF system is highly affected by the compressor speed ratio and fan speed ratio. Kang et al. [20] evaluated the performance of the HR-VRF system in the five different operation modes, cooling-only, cooling-main, heating-only, heating-main, and entire heat recovery operation mode. The test was performed under the specific experimental conditions inside the psychrometric calorimeter chamber. The COP in the cooling-main operation mode was 3.46, which was 10.9% higher than that in the cooling-only operation mode. The COP of the entire heat recovery operation mode was 146.5% higher than that in the cooling-only operation mode. Li and Wu [21] developed an energy simulation module for the HR-VRF system in the EnergyPlus program and evaluated energy features of the HR-VRF system. Also, the energy comparison between HP-VRF and HR-VRF was performed theoretically. Based on the simulation results, the HR-VRF system consumed about 6%~10% less power than the HP-VRF system. The HR-VRF and ground source heat pump (GSHP) systems were compared theoretically by using EnergyPro and eQUEST program, respectively, by Liu and Hong [22]. The simulation results showed that GSHP system was more energy efficient than the air source HR-VRF system for conditioning a small office building. GSHP system saved 9.4 − 24.1% of HVAC energy compared with the HR-VRF system with the standard rated refrigerant piping length. However, the main characteristics of the HR-VRF system in terms of the heat recovery operation mode were not considered in the paper.

2.2   Heat Pump Water Heater

Guo et al. [23] constructed an experimental set-up of air-source heat pump water heater system and developed a simulation model. Optimization analyses based on structural parameters, timing control pattern and thermostatic control pattern were performed to investigate the performance

characteristics. The daily average COP of the heat pump water heater system was 4.3, 3.2 and 2.6 for the summer, transitional season and winter, respectively. Fernandez et al. [24] evaluated the performance of the CO_2 heat pump water heater and investigated the effect of three environmental parameters on the overall COP and average capacity. It was concluded that the overall COP and average capacity are increased by facilitating a higher evaporating temperature and pressure as the ambient temperature was increased. Zhang et al. [25] tested and calculated the performance of the air source heat pump water heater. After evaluating the performance of the air source heat pump system, refrigerant charge amount, the thermal expansion valve (TXV) opening degree, the length of condensing coil pipe were optimized to enhance the baseline air source heat pump water heater. It was found that refrigerant charge amount played an important role in heat pump system performance. It was not only related to the climate condition, but also coupled with the TXV opening degree. They concluded that the heat pump capacity and water tank size should be properly matched in residential air-source heat pump water heater system. Morrison et al. [26] presented an experimental method of rating air-source heat pump water heaters and evaluated the heat pump performance during heat-up operation. They developed empirical correlations of the COP and power consumption of heat pump water heater system. Anderson and Morrison [27] investigated the performance of a solar-boosted heat pump water heater operating under full load and part load conditions in an outdoor experimental study. Whole tank heating, half tank heating and sort cycle testing were performed under the various outdoor weather conditions. They reported that the development of stratification within the tank had a significant effect on the heat pump capacity. Stene [28] carried out theoretical and experimental study for a residential brine-to-water CO_2 heat pump system for combined space heating and water heating over a wide range of operating conditions. The CO_2 heat pump was

evaluated in three different modes: space heating-only, domestic hot water heating-only and simultaneous space heating and domestic hot water heating. They showed that an integrated residential brine-to-water CO_2 heat pump system achieved higher seasonal performance factor than the most energy efficient brine-to-water heat pump system. Ji et al. [29] introduced a novel air-conditioning product that can achieve the multi-functions: space cooling, water heating and space heating. Waste heat recovery process was achieved by integrating a water-cooled condenser to the outdoor unit of a heat pump. They reported that average COP, of space heating-only, water heating-only and space cooling / water-heating were 2.72, 3.25 and 4.02, respectively.

2.3   Objective of Study

As seen in the literature, although experimental and theoretical studies on the HP-VRF system have been conducted extensively, there are a few studies on the HR-VRF system over the wide range of the working conditions through field performance tests. Plus, in terms of the heat pump water heater, most of the previous studies were conducted on the stand-alone water heating system using a heat pump. There are lack of the studies on combination of water heating and HR-VRF system in the open literature. In this study, the MFVRF system - which can provide space cooling, space heating and hot water simultaneously - was installed and fully instrumented in the actual office building to investigate the effects of hot water demand and the heat recovery operation mode on the MFVRF system performance during the heating and shoulder seasons.

3 Experimental Setup and Instrumentation

3.1 Floor Layout

The space and zoning layout for a MFVRF system are shown in Figure 3.1 and Figure 3.2. One outdoor unit was installed on the roof and was connected to the heat recovery units with three pipes. The maximum number of indoor units that can be connected is four for each heat recovery unit. The indoor units located in room A and room B and the water heating system were connected to the first heat recovery unit (HR 1). The indoor units, IU4, IU5, IU6 and IU7, were connected to the second heat recovery unit (HR 2).
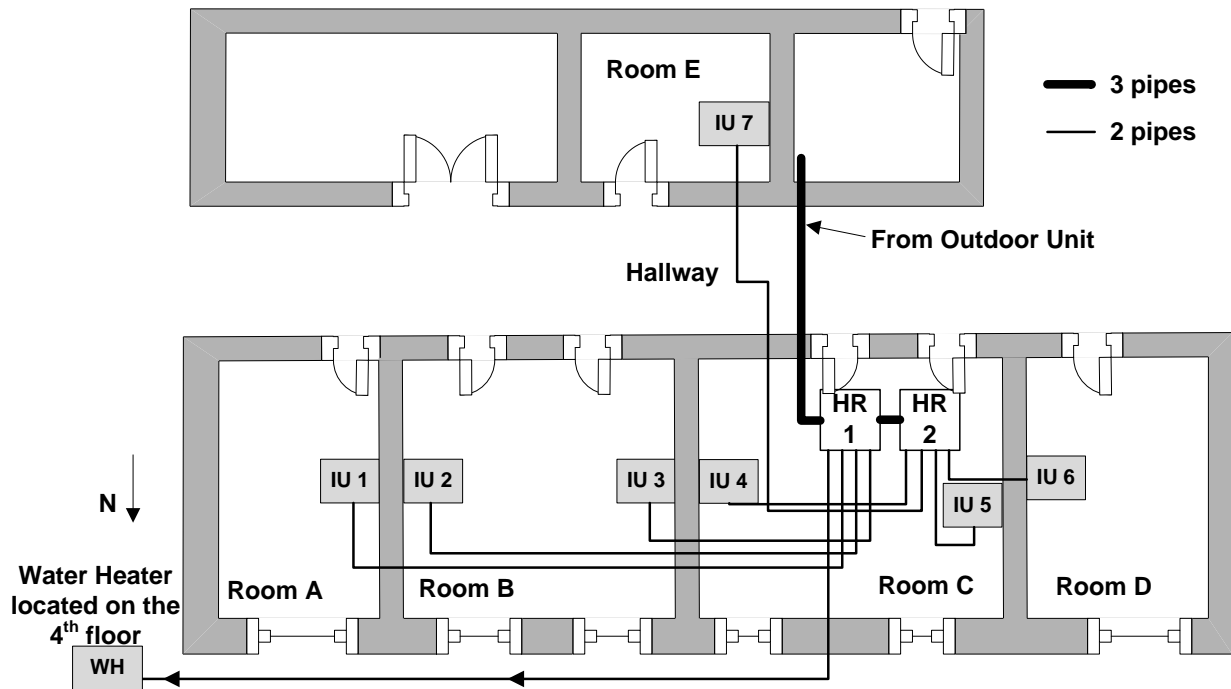
Figure 3.1: Space layout and zoning layout of a MFVRF system (3rd Floor)
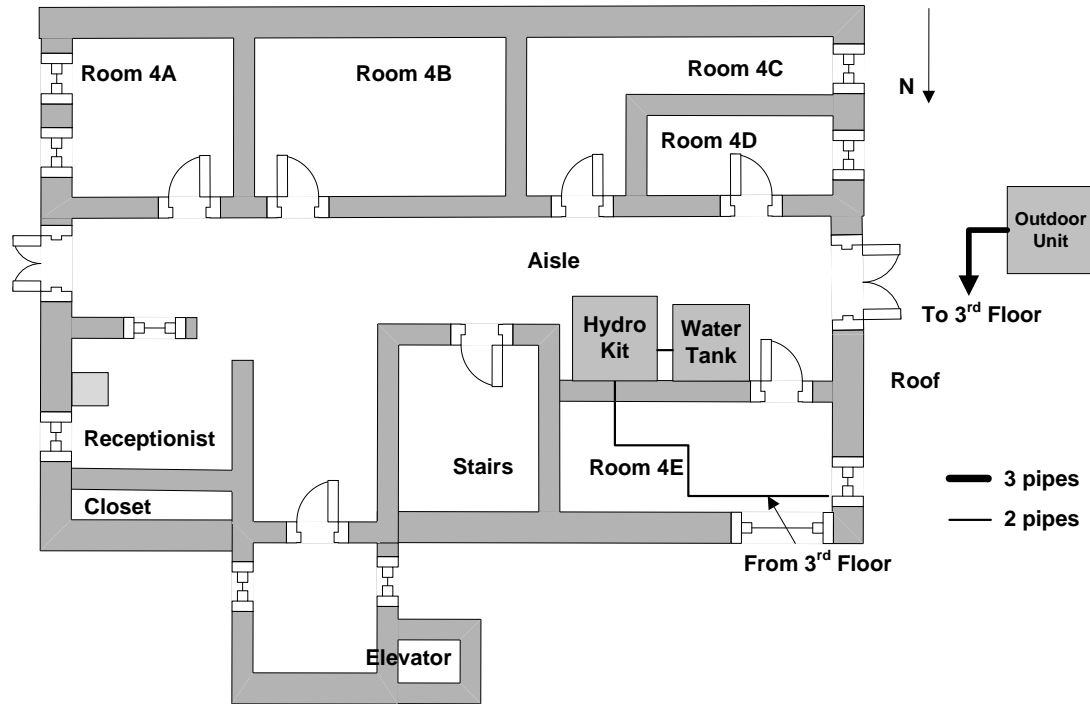
Figure 3.2: Space layout and zoning layout of a MFVRF system (4th Floor)

Figure 3.2 shows the layout of a fourth-floor and water heating system. The two pipes (gas and liquid pipe) from the heat recovery unit were connected to the water heating system. The water heating system and hot water tank were installed in front of room 4E.

Table 3-1 shows the internal heat gains and space area for each thermal zone. room E is located in the middle of the building and has high internal heat gains, which is mainly generated by office equipment. Moreover, room E is surrounded by the hallway of the building so that heat loss is considerably small. That means cooling may be required through the year in that room. Internal heat gains of room C are considerable higher than the other rooms because of a large number of occupants and a large amount of office equipment. If the outdoor temperature is not low subsequently, room C would require cooling year-round.

Table 3-1: Internal heat gains and area for each thermal zone

	Room A	Room B	Room C	Room D	Room E
Space area (m^2)	11.36	22.14	22.38	11.36	9.34
Number of occupants	1	5	7	1	1
Office equipment (W/m^2)	30.37	62.10	94.99	34.8	56.78
Lighting (W/m^2)	13.20	13.55	13.41	16.06	13.20

3.2   Multifunctional VRF System

Figure 3.3 shows a schematic drawing of the MFVRF. The system has four major components, OU, HRU, IUs and a water heating unit. OU consists of two compressors, a fixed and variable speed compressor, two finned tube heat exchangers, two propeller fans, two four-way valves, two electronic expansion valves, and a subcooling heat exchanger (SCHX). An inverter-driven compressor provides the variable refrigerant mass flow rate to the system — depending on the cooling or heating load of the thermal zones — by changing the compressor operation frequency. Instead, the constant speed compressor also runs in order to cover the higher cooling or heating loads than what the variable speed compressor can cover. The four-way valves located inside OU are used to change the refrigerant path based upon the operation mode of the system.
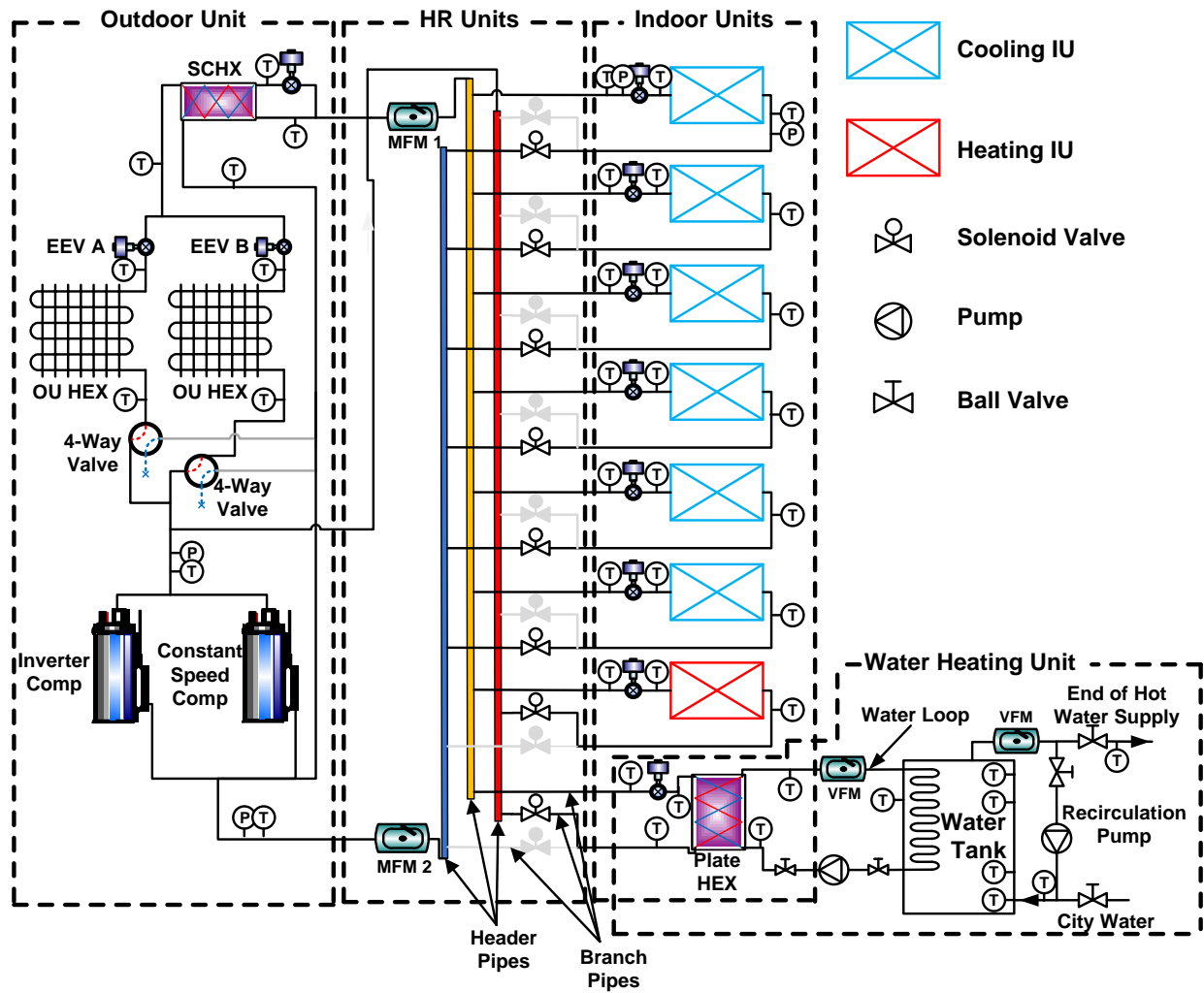
Figure 3.3: Schematic diagram of the MFVRF system

A HRU consists of header pipes, branch pipes, and solenoid valves. The solenoid valve, located in the branch pipe, controls the refrigerant flow path entering into each indoor unit, which changed the system operation mode. A water heating unit consists of a plate heat exchanger (PHX), an EEV, pumps and water tank. Water is circulating in the water loop to transfer heat from PHX to water tank.

3.2.1 Outdoor Unit

Table 3-2 shows the specifications of the OU and Figure 3.4 shows the picture of the OU installed on the roof. Inverter operation range of compressor was from 20 Hz to 120 Hz.

Table 3-2: Specifications of the outdoor unit

Cooling Capacity (kW)	Heating Capacity (kW)	Refrigerant
35.2	39.6	R410A
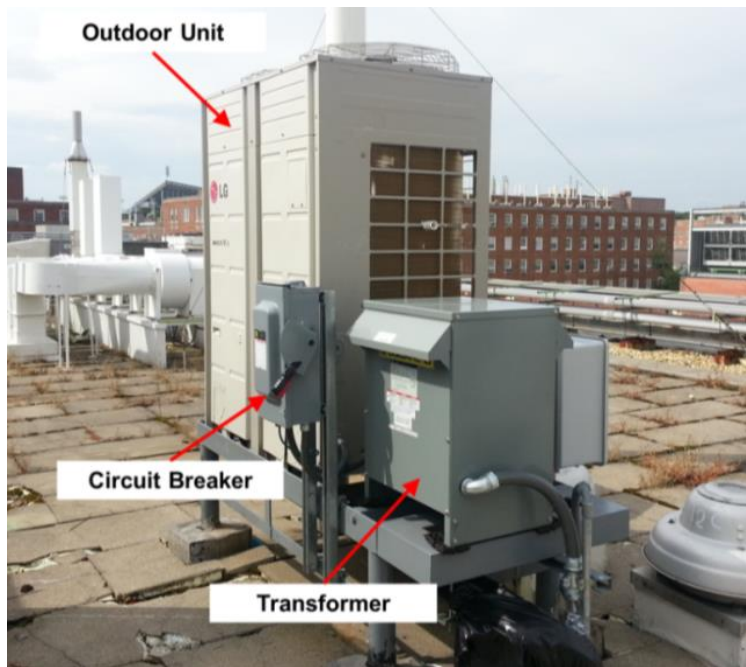
Figure 3.4: Outdoor unit

3.2.2 Indoor Units

Figure 3.5 shows the one of the indoor units installed in an office suite. Wall mounted indoor units were installed and thermostat was located below the each indoor unit. Each IU was equipped with a finned-tube heat exchanger, an EEV and a fan. The EEV was used to control the

refrigerant mass flow rate to react to changes in the zone's heating/cooling loads. The fan was used to force the air through the heat exchanger. Table 3-3 shows the specification, type and location of the indoor units. The size of the indoor unit was decided based on the peak load through the year.
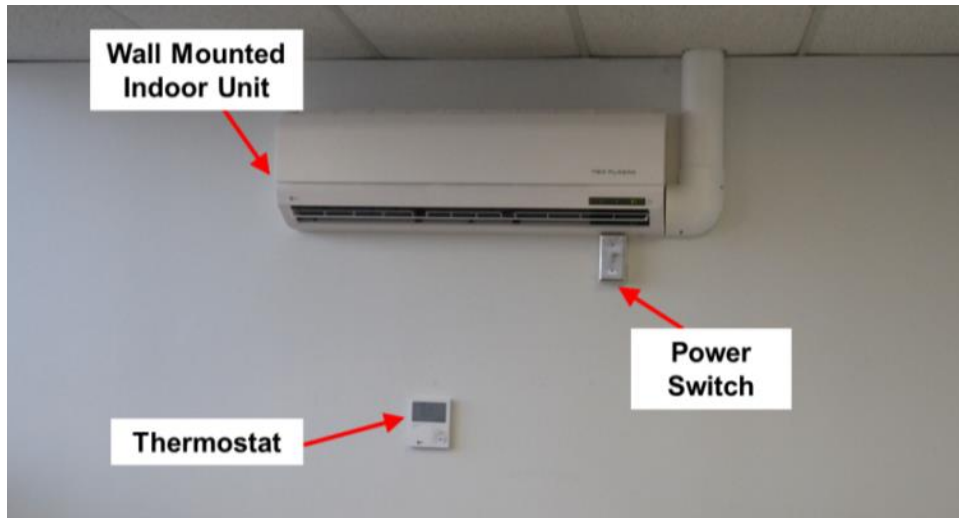
Figure 3.5: One of the indoor units with thermostat

Table 3-3: Specification, type and location of the indoor units

Indoor Unit	Cooling Capacity (kW)	Heating Capacity (kW)	Type of Indoor Unit	Zone	HRU Connected
IU 1	2.2	2.5		Room A	
IU 2	3.6	4.0		Room B	HR 1
IU 3	3.6	4.0		Room B	
IU 4	5.6	6.3	Wall Mounted	Room C	
IU 5	5.6	6.3		Room C	HR 2
IU 6	2.2	2.5		Room D	
IU 7	2.2	2.5		Room E	

3.2.3 Heat Recovery Units

Figure 3.6 shows the two heat recovery units installed in the ceiling of the room C. The heat recovery units were connected in succession with three pipes. Since there are four connection ports in the one heat recovery unit, four indoor units can be connected at once.
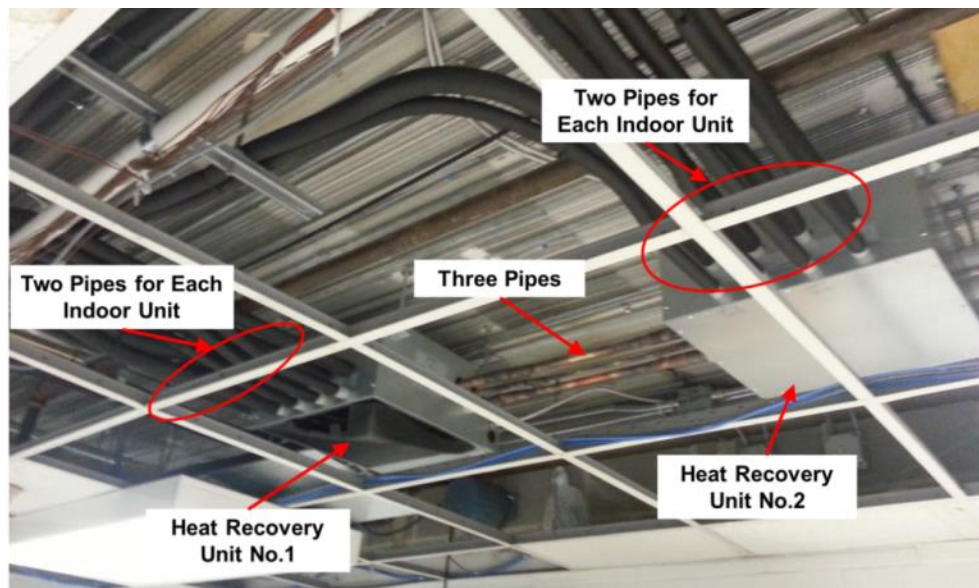
Figure 3.6: Heat recovery units

3.2.4 Water Heating System

The water heating system connected to the MFVRF system is an indirect water/heating system which uses water as a medium. The water heating system consists of a plate heat exchanger (PHX), an EEV, pumps and water tank. When the water flows passed through the PHX, it absorbs the heat rejected by the refrigerant and is fed to the water tank. Schematic drawing of the water heating system is shown in Figure 3.7. For better hot water temperature stratification, a recirculation pump was installed, and in order to simulate the actual hot water demand in this study, a service pump and actuator valve were also installed to supply the hot water.
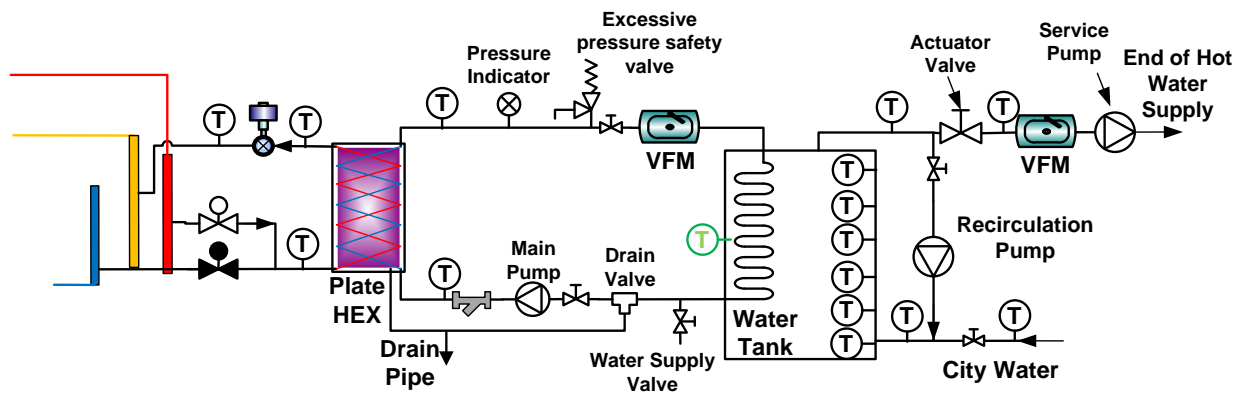
Figure 3.7: Schematic drawing of the water heating system

Table 3-4: Specification of the water heating system

Cooling Capacity (kW)	14.1
Heating Capacity (kW)	15.9
Heat Exchanger	Brazed Plate Type
Refrigerant	R410A

Figure 3.8 show the picture of the water heating system installed in front of the room 4E. Water tank temperature sensors were immersed in the water tank to control the water heating. When the water tank temperature sensor senses low water temperature, the water heating system turns on the main pump, which located between the water heating system and water tank. EEV regulates the refrigerant mass flow rate based upon the water tank temperature. An emergency shut-off valve and expansion tanks are installed for safety. Since there was no actual hot water demand, the hot water was drained out according to artificial hot water demand profile. The installation picture of the drain pump and water tank is shown in Figure 3.9.
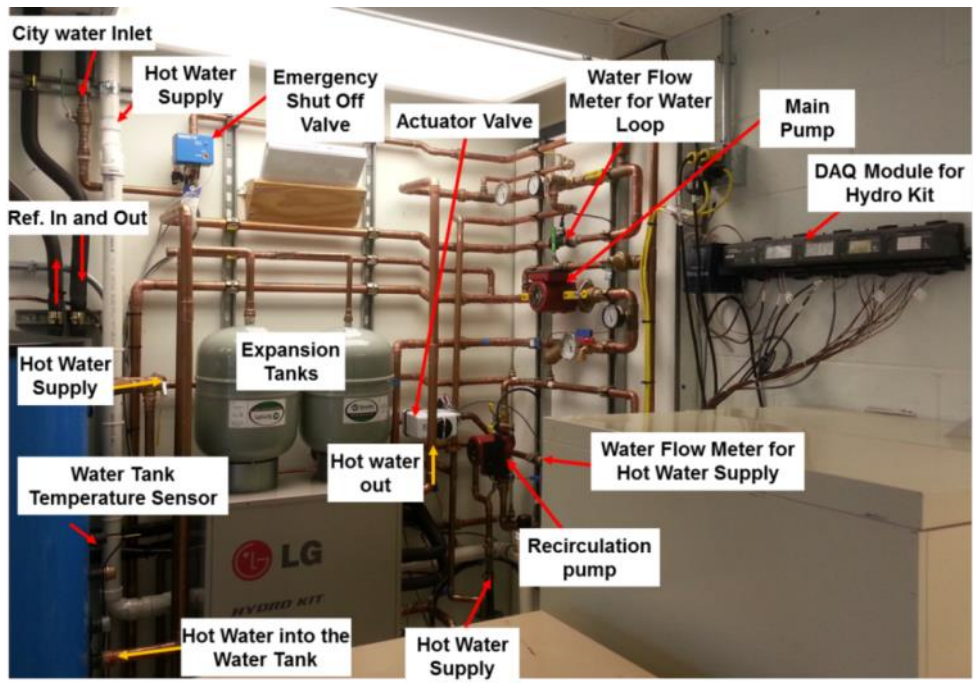
Figure 3.8: Water heating system

Figure 3.9: Drain pump and water tank

3.3 Instrumentation and Measurement

3.3.1 Temperature and Relative Humidity Measurement

A total of ten thermocouples were attached to the surface of the refrigerant pipes in the outdoor unit to analyze the cycle characteristics. The detailed locations of the thermocouples are shown in Figure 3.10.
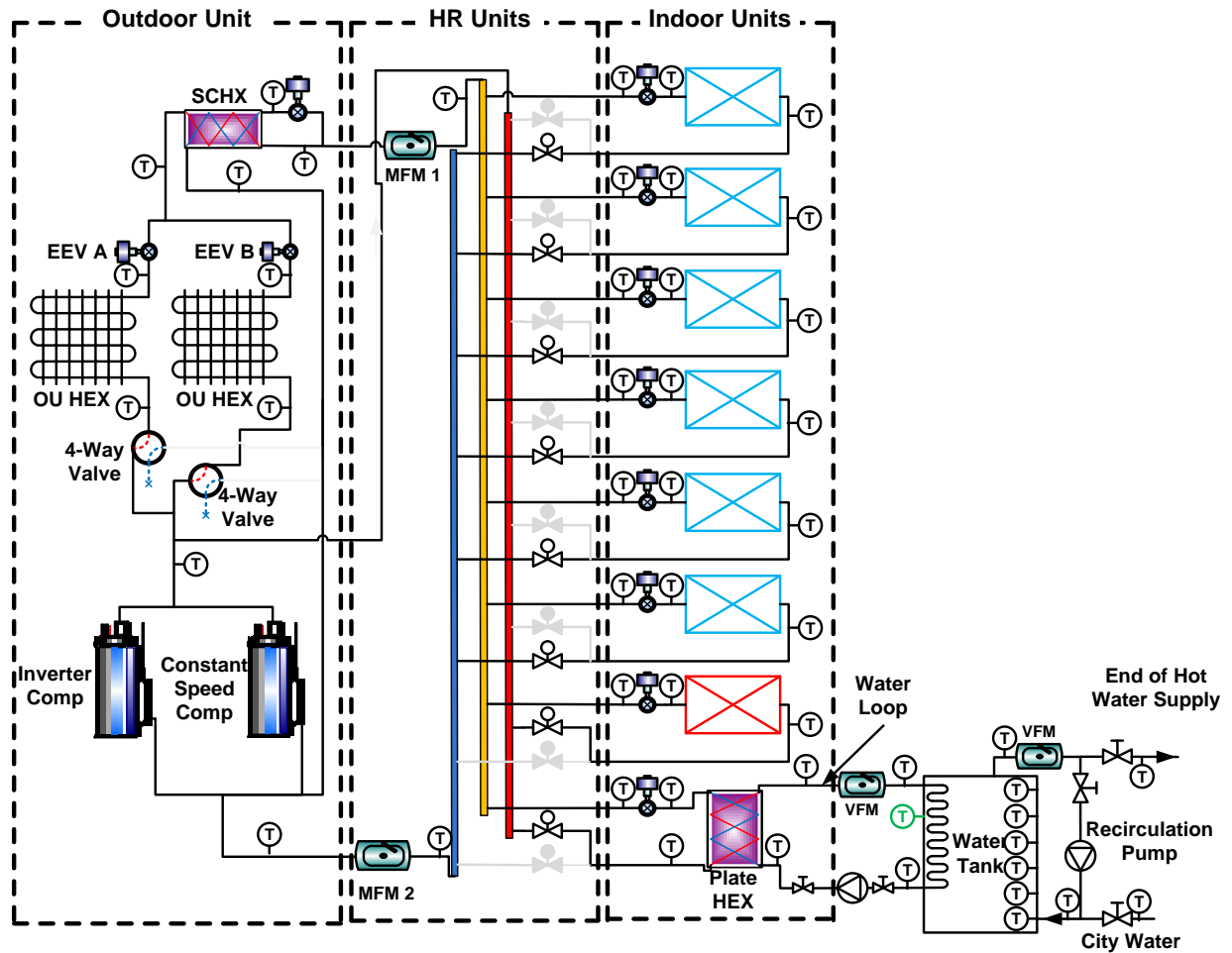
Figure 3.10: Temperature measurement location
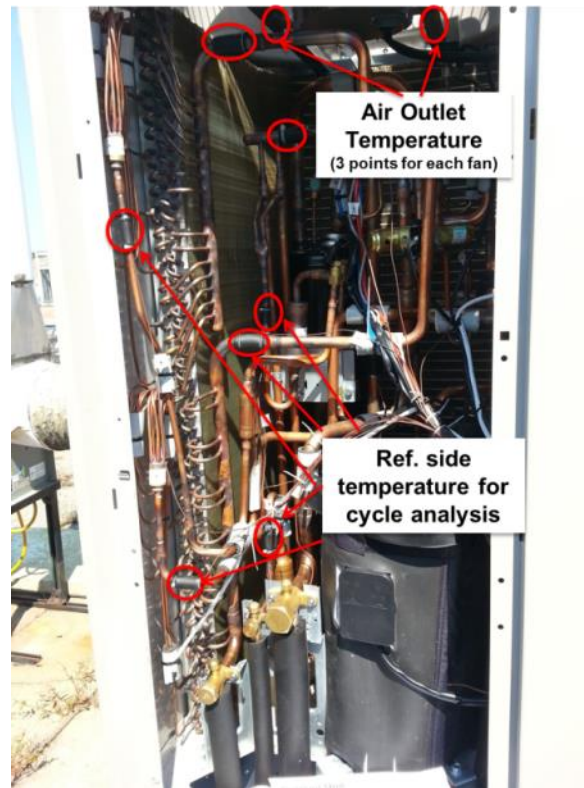
Figure 3.11: Air- and refrigerant-side temperature measurement location of OU

Figure 3.11 depicts the location of the thermocouples in the OU. Because there are issues of shielding regarding air outlet temperature measurement, we placed T-type thermocouples just below the outdoor unit fan instead of top of the outdoor unit fan. Figure 3.12 shows the air inlet temperature measurement points of outdoor unit. Eight T-type thermocouples were place around 10 cm spacing from the heat exchanger and those were shield against the heat radiation and rain.
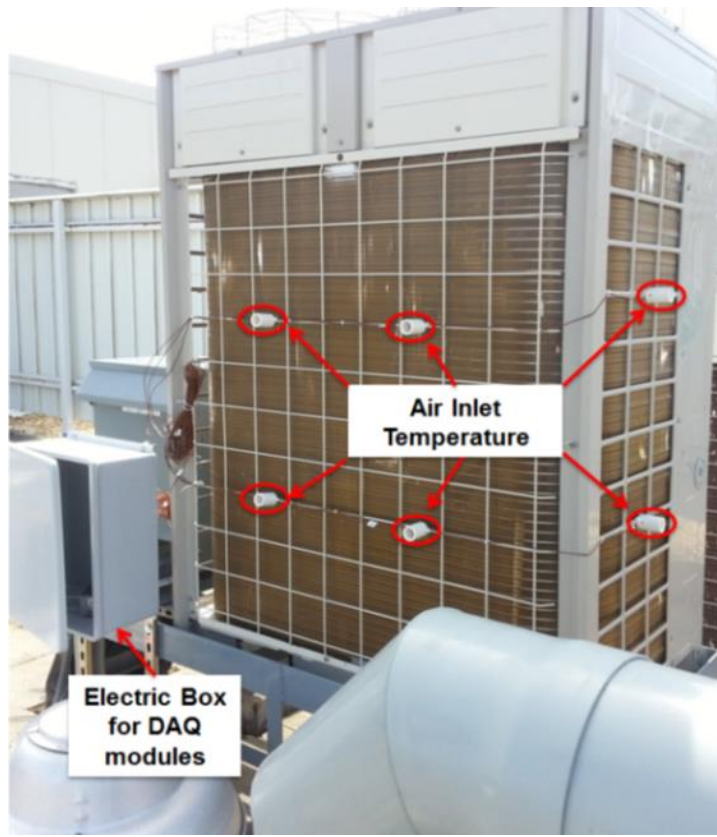
Figure 3.12: Air inlet temperature measurement location of outdoor unit

There are three head pipes inside the each heat recovery unit. Temperatures of the liquid and gas refrigerants were measured using T-type thermocouples. Three thermocouples were installed to measure the refrigerant temperature on the pipe surface for each indoor unit. One thermocouple was attached to the refrigerant pipe surface just before EEV, another was attached after EEV, and the third was attached to the refrigerant pipe after the heat exchanger. Figure 3.13 shows the refrigerant-side temperature measurement location of one of the indoor unit.
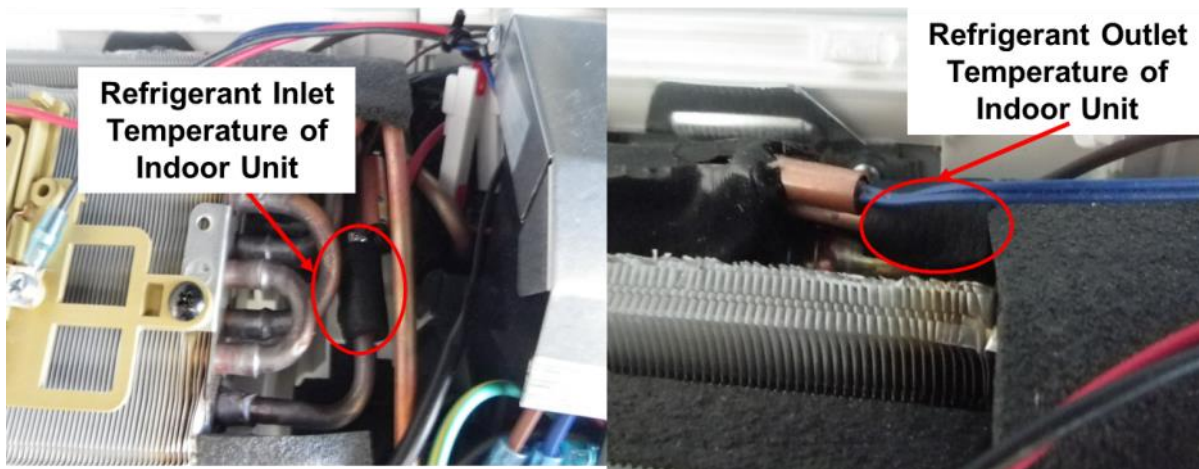
Figure 3.13: Refrigerant-side temperature measurement location of indoor unit
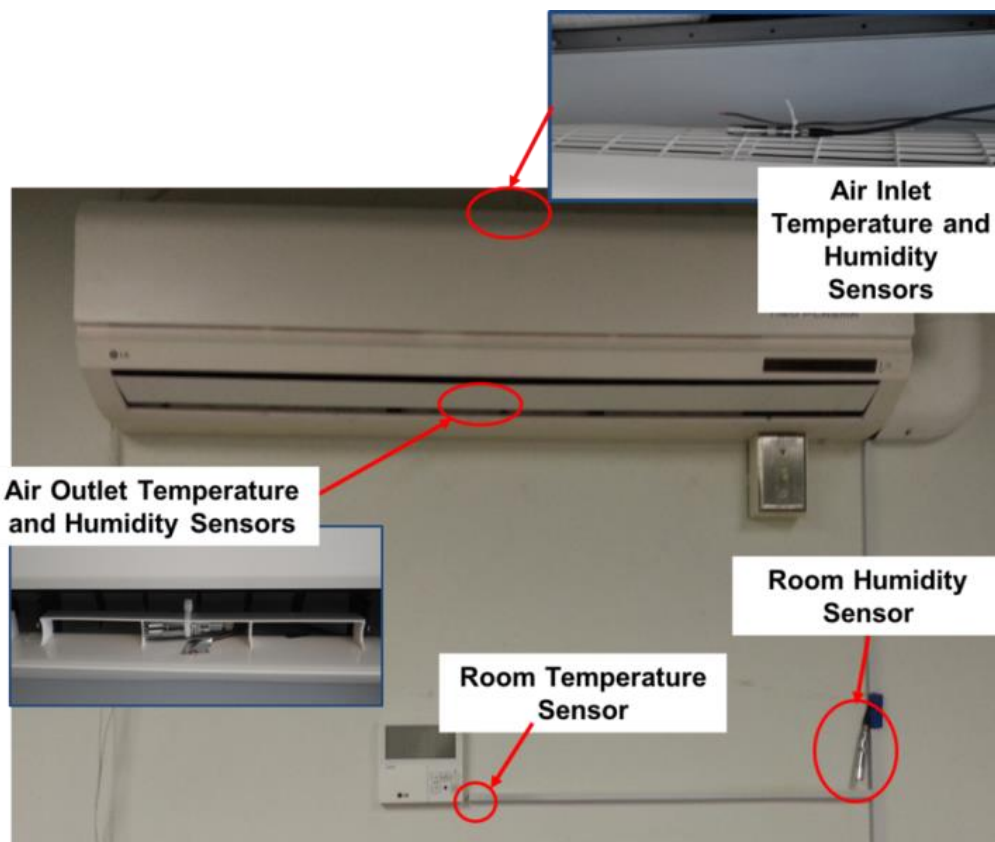
Figure 3.14: Air-side measurement location for indoor unit and room conditions

Figure 3.14 shows the location of temperature and humidity sensors for the indoor unit as well as

the room conditions. T-type thermocouples and relative humidity sensors were installed for each

air discharge unit, and the suction grille of each indoor unit, to measure the air inlet and outlet temperature and relative humidity. The room temperature was measured precisely next to the thermostat. The relative humidity of the room was measured 20 cm from the thermostat.
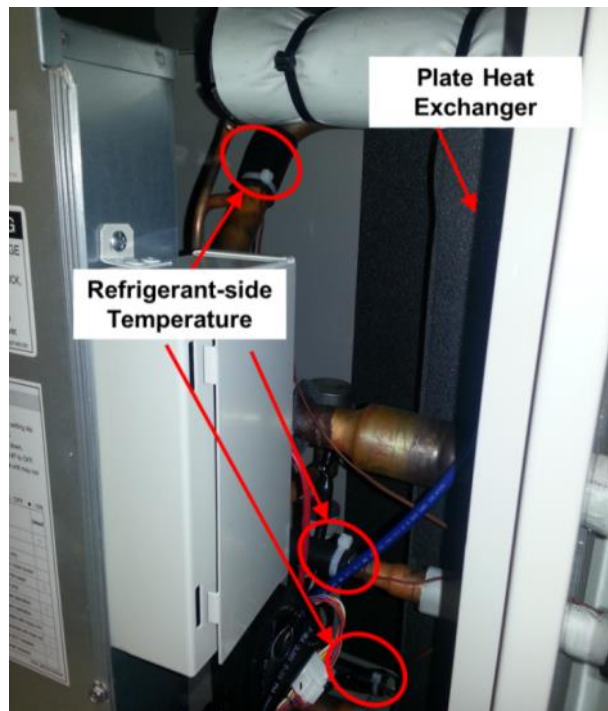
Figure 3.15: Refrigerant-side temperature measurement location for water heating system

Fifteen thermocouples were installed to evaluate the performance of the water heating system. Three T-type thermocouples were attached to the pipe surface to measure the refrigerant temperature of the water heating system, as shown in Figure 3.15. Measurement locations for the water-side of the water heating system are shown in Figure 3.16.
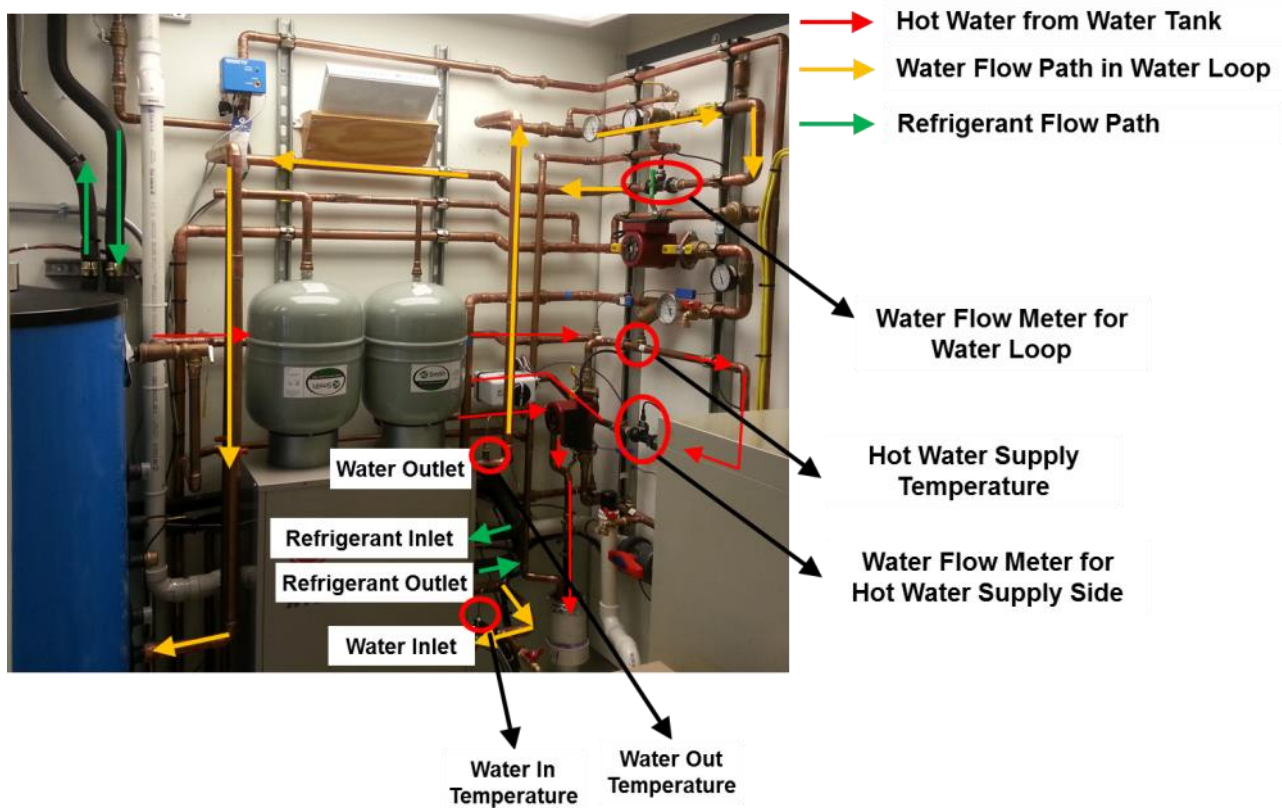
Figure 3.16: Measurement location of water heating system

The water temperature entering and leaving the water heating system was measured by T-type in-stream thermocouples. Supply hot water temperature was also measured using the T-type thermocouple. The hot water temperature of the water tank was measured at six heights within the water tank by a multiple junction thermocouple probe inserted along the axis of the tank, as shown in Figure 3.17. Room air temperature and relative humidity measurement locations in the office suite are shown in Figure 3.18. Outdoor conditions, temperature and relative humidity are measured underneath the outdoor unit in order to shield them against the radiation and the rain.
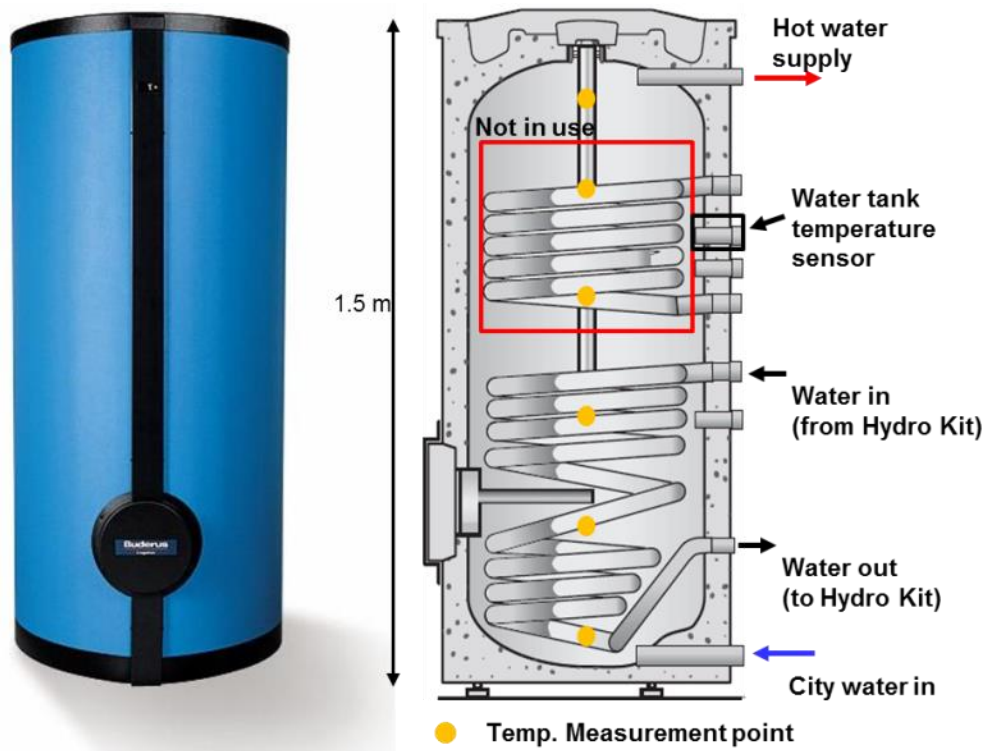
Figure 3.17: Water tank image and thermocouple locations in the water tank
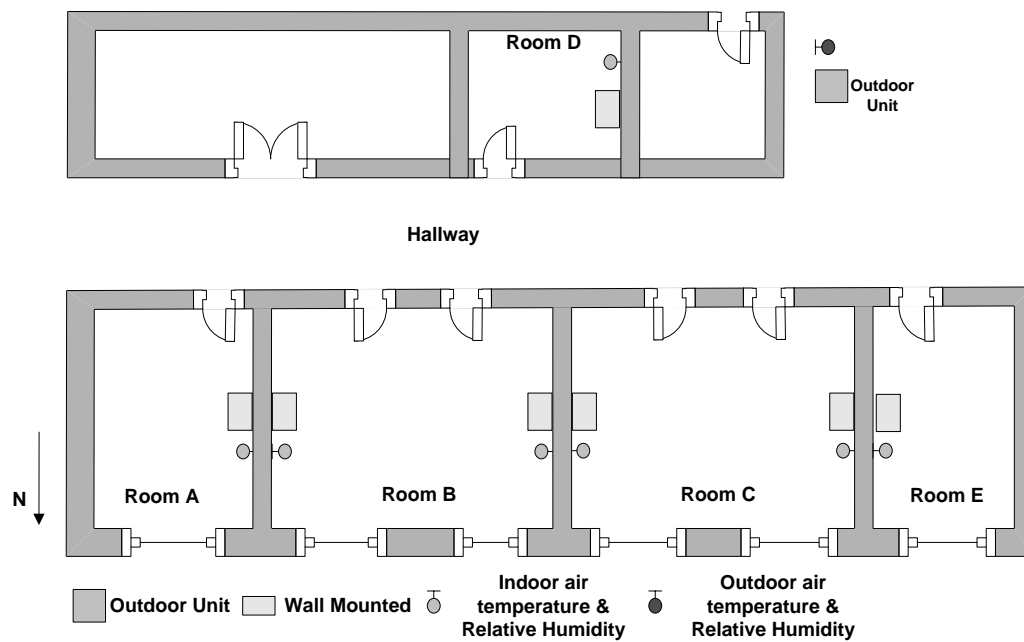
Figure 3.18: Measurement locations for room and outdoor conditions

3.3.2 Pressure Measurement

Built-in pressure sensors recorded compressor suction and discharge pressures. Additionally, two pressure transducers were installed in one of the indoor units as shown in Figure 3.19. Figure 3.20 shows the picture of the pressure transducers installed in the one indoor unit.
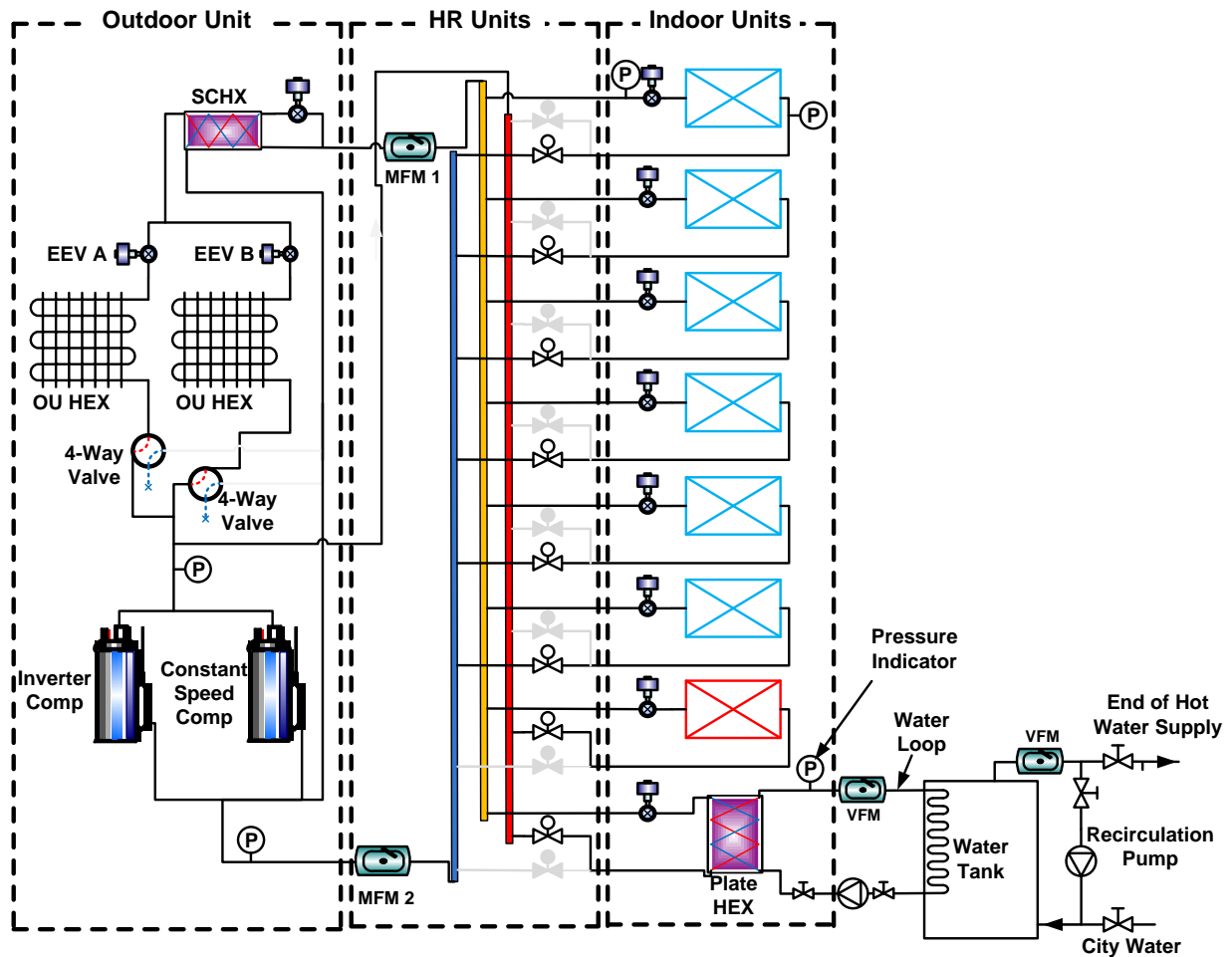
Figure 3.19: Pressure measurement locations
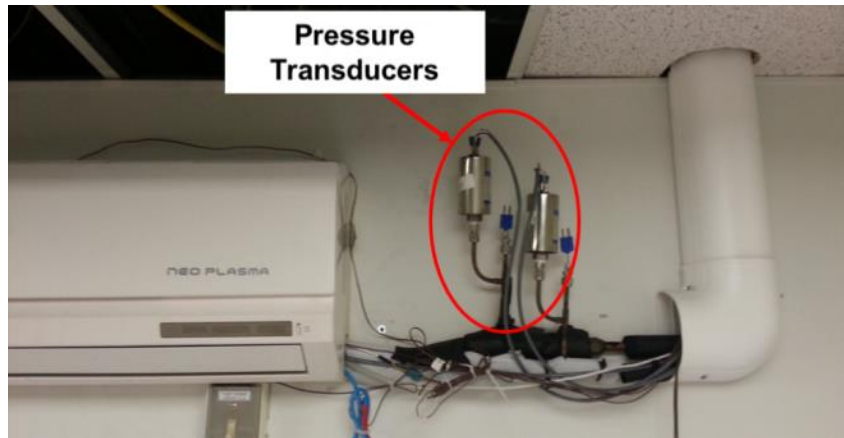
Figure 3.20: Refrigerant-side pressure measurement locations for indoor unit

3.3.3 Refrigerant- and Water-Flow Rate Measurement

Two Coriolis mass flow meters were installed to measure the refrigerant mass flow rates. One was installed in the liquid line (MFM 1), the other was located in the vapor line (MFM 2), as shown in Figure 3.19. Figure 3.21 shows the picture of the two Coriolis mass flow meters installed in the refrigerant side. Since the refrigerant mass flow meter is relatively expensive device, individual mass flow rate was calculated using the orifice equation.

Figure 3.21: Photos of Coriolis mass flow meters in refrigerant-side

Two volumetric flow meters were installed to measure the water flow rates. One was installed in the water loop: the other was installed in the hot water supply side. Based on the water flow rate for the hot water supply-side, an actuator valve-on and –off control scheme was developed. Figure 3.22 shows the picture of the water flow meters.
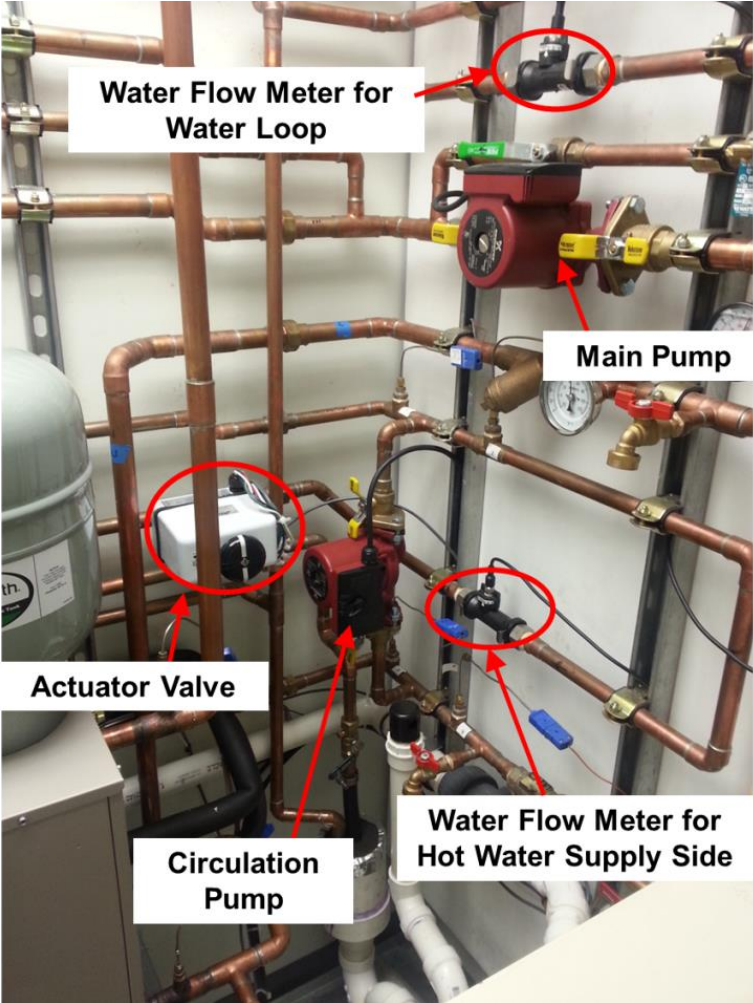
Figure 3.22: Water flow meters in water-side

3.3.4 Power Consumption and Line Voltage Measurement

Two watt meters were installed to measure the power consumption of the MFVRF system. One meter is for the total power consumption of the outdoor unit, which includes the compressor, fan motors and electronic expansion valves and control unit. In addition to the outdoor unit, the total power consumption of the seven indoor units, two heat recovery units and water heating system were measured with the separate watt meter as shown in Figure 3.23.
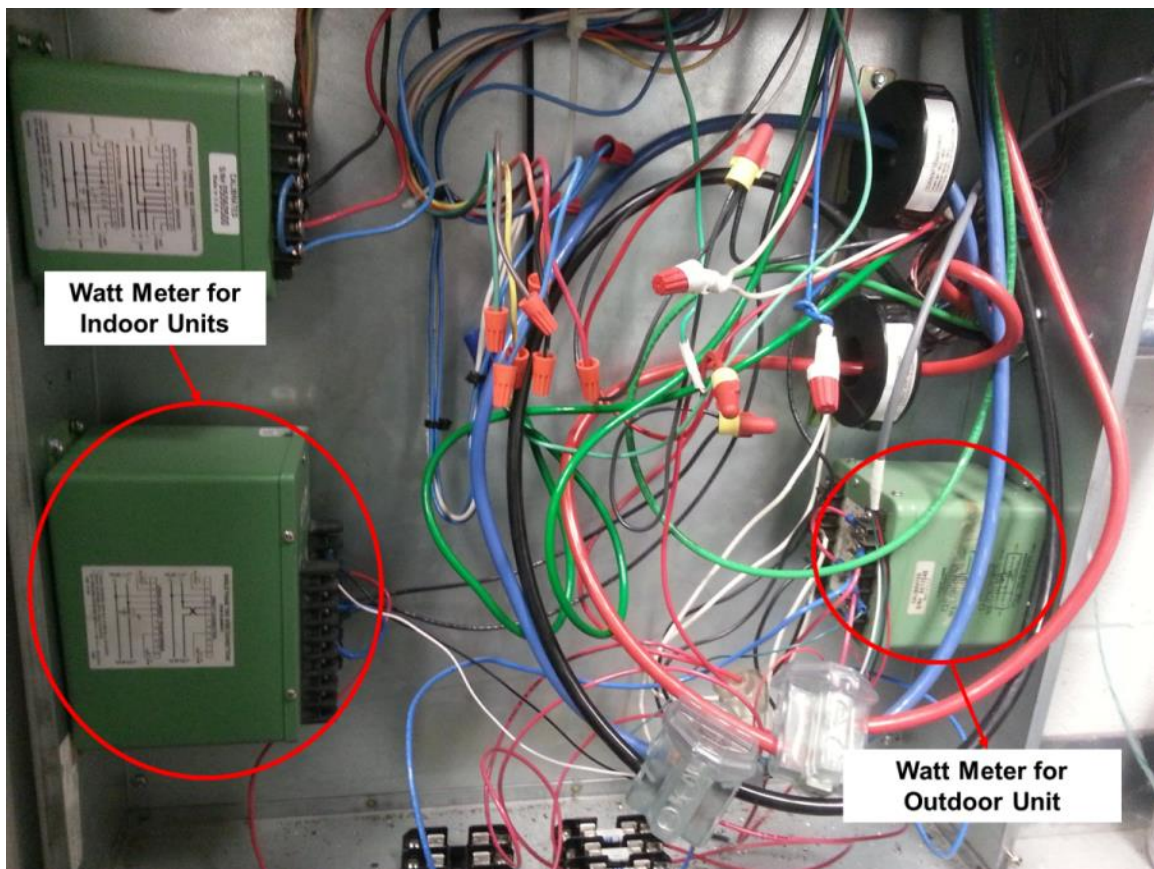
Figure 3.23 : Watt meters for power consumption measurement

3.3.5 Data Acquisition System
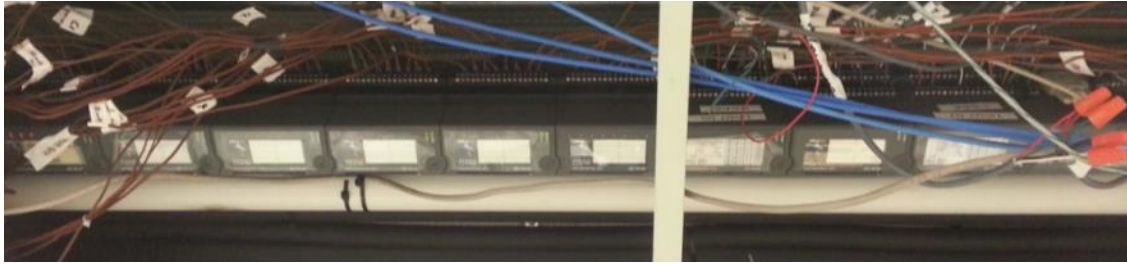
(a) DAQ modules located on the 3rd floor

(b) DAQ modules located on the 4th floor
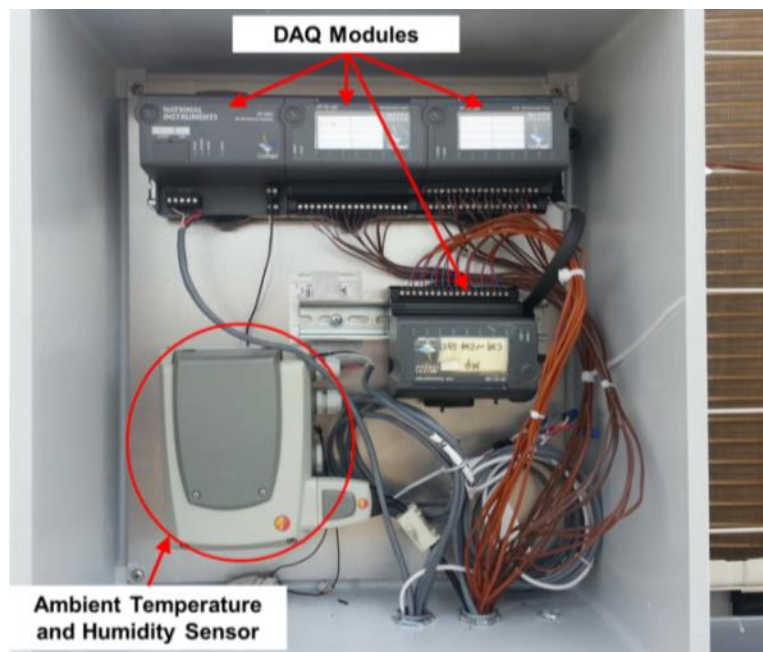
(c) DAQ modules located on the roof

Figure 3.24 : DAQ modules for data acquisition, (a) DAQ modules on the 3rd floor, (b) DAQ modules on the 4th floor, (c) DAQ modules on the roof

Since the data points for outdoor unit, indoor units and water heating system are far away apart, FieldPoint modules were placed into three locations near the data point. One set of DAQ module was installed on the ceiling of the third-floor for the indoor units, another was installed next to the water heating system for the water-side measurement, and the last one was located on the roof for the outdoor unit and outdoor weather conditions, as shown in Figure 3.24 (a), (b), and (c), respectively. In addition to these measurements, the real-time system information, such as the EEV opening, thermostat "ON/OFF" etc, were recorded at one minute intervals throughout the local MFVRF system network.

3.3.6   Uncertainty Analysis

Total uncertainty is comprised of systematic uncertainty and random uncertainty which is defined as shown in Equation 3-1.

$$\omega_{total} = \omega_{sys} + \omega_{rand} \qquad\qquad \text{Equation 3-1}$$

Random uncertainty is the standard deviation for each test, and systematic uncertainty is shown in Equation 3-2.

$$\omega_F = \sqrt{\left(\frac{\partial F}{\partial x_1}\omega_{x_1}\right)^2 + \left(\frac{\partial F}{\partial x_2}\omega_{x_2}\right)^2 + \cdots + \left(\frac{\partial F}{\partial x_n}\omega_{x_n}\right)^2} \qquad \text{Equation 3-2}$$

where F is the target parameter, and x_n is the variable which the target parameter is dependent on. The maximum uncertainty values of the cooling and heating capacity of the MFVRF system,

daily performance factor (DPF), and the power consumption are shown in Table 3-5. And the accuracies of the sensors are provided in Table 3-6.

Table 3-5: Experimental uncertainties

Power consumption	±0.5%
Cooling and heating capacity	±8% of calculated value
DPF	±9% of calculated value

Table 3-6: Accuracies of the sensors

Sensor	Accuracy
T-type thermocouples (range: -200 – 350 ℃)	±0.5 ℃
Pressure transducer (range: 0 – 6,770 kPa)	±6.34 kPa
Pressure transducer (range: 0 – 3,339 kPa)	±4.21 kPa
Relative humidity sensor (range: 0% – 100%)	±3.0%
Mass flow meter 1 (range: 3 – 457.5 g s-1)	±0.2% of flow rate
Mass flow meter 2 (range: 0 – 450 g s-1)	±0.2% of flow rate
Watt meter (range: 0 – 4 kW)	±0.2% of full scale
Watt meter (range: 0 – 40 kW)	±0.5% of full scale

4 Evaluation Methodology

4.1 Refrigerant Mass Flow Rate

In order to evaluate the heating and cooling capacities of the indoor units and water heating system, the refrigerant enthalpy method [9, 30] was used. Total refrigerant mass flow rates for the heating and cooling modes were obtained from the two Coriolis mass flow meters. One meter was installed in the liquid pipe, the other was installed in the vapor pipe. In the heating-only operation mode, the mass flow meter 1 (MFM 1), located in the liquid line, measures the total refrigerant mass flow rate of the heating operated indoor units.
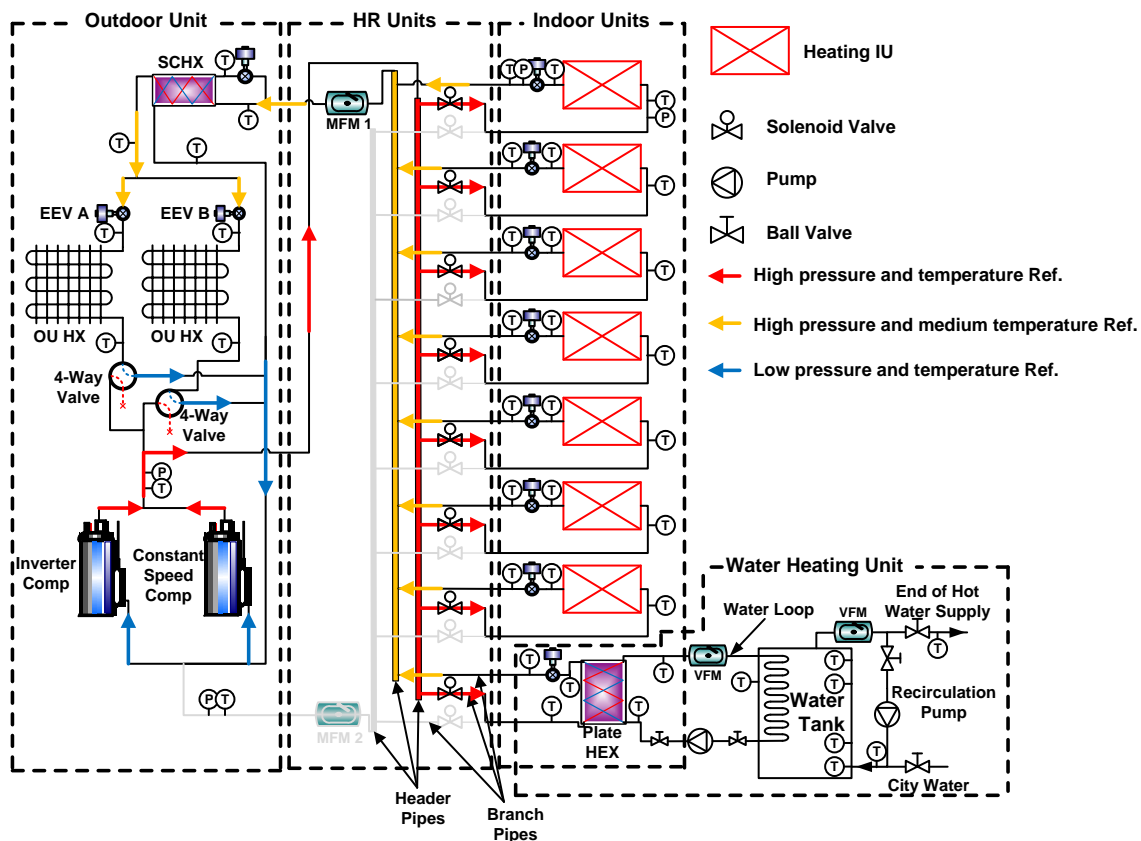
Figure 4.1: Refrigerant flow path in the heating-only operation mode

Figure 4.1 shows the refrigerant flow path in the heating-only operation mode. All discharge refrigerants enter the heat recovery units and are distributed to each indoor unit. After releasing the heat to the each thermal zone, liquid refrigerant flows back to the heat recovery unit in the liquid line. Figure 4.2 shows the refrigerant flow path in the heating-based operation mode. Two indoor units are operating in the cooling mode and the other indoor units and water heating system are working in the heating mode, as depicted in Figure 4.2.
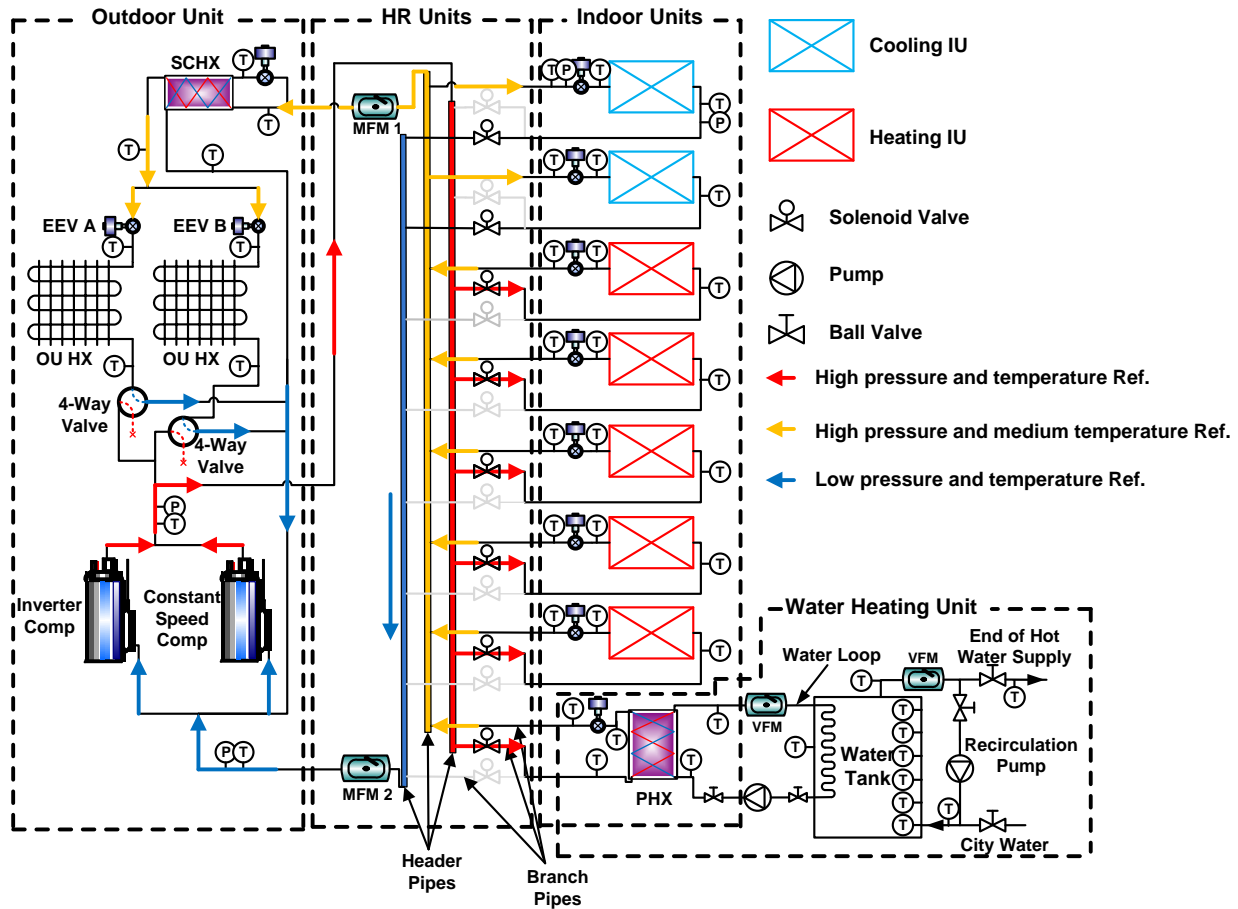
Figure 4.2: Refrigerant flow path in the heating-based operation mode

The mass flow rate obtained from Equation 4-1 was used to calculate the heating capacity for all indoor units and water heating system, because the total refrigerant flow discharged from the

compressor was divided in the liquid header pipe of the heat recovery unit. The mass flow meter

2 (MFM 2) measures the total refrigerant mass flow rate of the cooling operated indoor units.

$$\dot{m}_{total,heating} = \dot{m}_1 + \dot{m}_2 \qquad\qquad \text{Equation 4-1}$$

$$\dot{m}_{total,cooling} = \dot{m}_2 \qquad\qquad \text{Equation 4-2}$$

The individual refrigerant mass flow rate of the indoor unit was determined by the Equation 4-3.

Similar to the literature [17, 30], the mass flow rate passing through the expansion valve is

calculated as a function of the cross section area of the EEV (A), flow coefficient (c_D),

refrigerant inlet density (ρ), and the pressure drop across the EEV (ΔP). Flow coefficient is

obtained from the manufacturer data.

$$\dot{m}_i = C_D \cdot A \cdot \sqrt{2 \cdot \Delta P \cdot \rho} \qquad\qquad \text{Equation 4-3}$$

4.2   Performance of MFVRF System

Individual cooling capacity of each indoor unit operating in the cooling mode was calculated by

Equation 4-4.

$$\dot{Q}_{c,i} = \dot{m}_i \cdot \left(h_{c,i,o} - h_{c,i,i} \right) \qquad\qquad \text{Equation 4-4}$$

where $\dot{m}_i$ is the refrigerant mass flow rate for each indoor unit and $h_{c,i,o}$ and $h_{c,i,i}$ are the outlet and inlet refrigerant enthalpy of the ith indoor unit heat exchanger. The total cooling capacity of the indoor units operating in the cooling mode was obtained by Equation 4-5.

$$\dot{Q}_{c,T} = \sum_{i=1}^{7} \dot{m}_i \cdot \left(h_{c,i,o} - h_{c,i,i} \right)$$

Equation 4-5

where $\dot{Q}_{c,T}$ is the total cooling capacity of the indoor units in the cooling mode.

Similarly, heating capacity of the individual indoor unit operating in the heating mode was calculated by Equation 4-6.

$$\dot{Q}_{h,i} = \dot{m}_i \cdot \left(h_{h,i,i} - h_{h,i,o} \right)$$

Equation 4-6

The total heating capacity of the indoor units operating in the heating mode was defined as the Equation 4-7.

$$\dot{Q}_{h,T} = \sum_{i=1}^{7} \dot{m}_i \cdot \left(h_{h,i,i} - h_{h,i,o} \right)$$

Equation 4-7

The water heating system was equipped with a plate heat exchanger to transfer heat between the refrigerant and water. The water coming from the plate heat exchanger releases the heat to the water tank. Water-side capacity was calculated by Equation 4-8.

$$\dot{Q}_{WH,w} = c_p \cdot \dot{m}_w \cdot \left(T_{w,out} - T_{w,in}\right)$$

$\qquad$ Equation 4-8

where $\dot{m}_w$ is the water mass flow rate obtained from the water flow meter installed between the

water heating system and the water tank, c_p is the specific heat capacity of water, and $T_{w,out}$ and

$T_{w,in}$ are the outlet and inlet water temperatures of the plate heat exchanger, respectively.

Refrigerant-side capacity is defined by multiplying the refrigerant mass flow rate by the inlet and

outlet enthalpy difference, which is shown in Equation 4-9.

$$\dot{Q}_{WH,r} = \dot{m}_{WH,ref} \cdot \left(h_{ref,in} - h_{ref,out}\right)$$

$\qquad$ Equation 4-9

where $\dot{m}_{WH,ref}$ is the refrigerant mass flow rate of water heating system, and $h_{ref,out}$ and

$h_{ref,in}$ are the outlet and inlet refrigerant enthalpy in the plate heat exchanger, respectively. Part-

load ratio (*PLR*) is used to describe the capacity of air conditioning equipment under non-

nominal condition. *PLR* is defined as the ratio of the actual capacity to available capacity. The

PLR of the MFVRF system in the heating-only and heating-based operation mode was calculated

by Equation 4-10 and Equation 4-11, respectively.

$$PLR_{heating,only} = \frac{\sum \dot{Q}_{h,T} + \dot{Q}_{WH,w}}{\dot{Q}_{heating,rated}}$$

$\qquad$ Equation 4-10

$$PLR_{heating,based} = \frac{\sum \dot{Q}_{h,T} + \dot{Q}_{WH,w} + \sum \dot{Q}_{c,T}}{\dot{Q}_{heating,rated}}$$

$\qquad$ Equation 4-11

45

Equation 4-12 shows the total power consumption of the MFVRF system.

$$\dot{W} = \dot{W}_{OU} + \dot{W}_{IUs} + \dot{W}_{pump}$$ Equation 4-12

where $\dot{W}_{OU}$ is the power of the outdoor unit, $\dot{W}_{IUs}$ is power of the indoor units and $\dot{W}_{pump}$ is the pump power of the water heating system. Power consumption by the outdoor unit was measured directly by a watt meter, which includes the compressor power, fan power and controller power in the outdoor unit. Total power consumption by the indoor units, heat recovery units and water heating system is measured by another watt meter, which includes thermostats, indoor units' fan motor, controller and water pump.

Daily performance factor (DPF) was used to evaluate the performance of the MFVRF system. DPF is defined as the Equation 4-13.

$$DPF = \frac{\sum \dot{Q}_{h,T} \cdot t + \dot{Q}_{WH,w} \cdot t + \sum \dot{Q}_{c,T} \cdot t}{\sum \dot{W} \cdot t}$$ Equation 4-13

where t is the testing time.

Because there is no actual hot water demand in the installation site, hot water consumption was estimated based on the statistical data [31]. Hot water demand was controlled by multiplying the single-family daily hot water demand by the number of households. Table 4-1 shows the single-family home daily hot water consumption by end use. Total hot water consumption for single-

family per day is about 65.2 gal. The structure and lifestyle of a typical family cause hot water consumption demand patterns to fluctuate widely in both magnitude and time distribution. Hourly hot water load profile was found [32], as shown in Table 4-2, and hourly hot water load was calculated by multiplying the total hot water consumption per day and the fraction for the hour.

Table 4-1: Single-family home daily hot water consumption by end use

End Use	Clothes Washer	Shower	Faucet	Bath	Dishwasher	Leaks	Total
Household Use (gal/day)	10.1	16.4	22.4	10.9	2.3	3.1	65.2

Table 4-2: Daily domestic hot water load profile

Time of Day	Daily fraction
00:00 ~ 01:00	0.0085
01:00 ~ 02:00	0.0085
02:00 ~ 03:00	0.0085
03:00 ~ 04:00	0.0085
04:00 ~ 05:00	0.0085
05:00 ~ 06:00	0.0100
06:00 ~ 07:00	0.0750
07:00 ~ 08:00	0.0750
08:00 ~ 09:00	0.0650
09:00 ~ 10:00	0.0650
10:00 ~ 11:00	0.0650
11:00 ~ 12:00	0.0460
12:00 ~ 13:00	0.0460
13:00 ~ 14:00	0.0370
14:00 ~ 15:00	0.0370
15:00 ~ 16:00	0.0370
16:00 ~ 17:00	0.0370
17:00 ~ 18:00	0.0630
18:00 ~ 19:00	0.0630
19:00 ~ 20:00	0.0630
20:00 ~ 21:00	0.0630
21:00 ~ 22:00	0.0510
22:00 ~ 23:00	0.0510
23:00 ~ 24:00	0.0085

5   Experimental Results

The field performance test of the MFVRF system was conducted during a wide range of outdoor weather conditions for the heating and shoulder seasons. Operating characteristics of heat recovery operation mode and the benefit of the water heating system were experimentally investigated based on the eight test conditions, shown in Table 5-1. Three hypothetical test conditions, tests No. 5, 6 and 7, aimed at representing typical MFVRF system use in a building were investigated. Data was monitored and collected for seven days a week from 6 a.m. - 8 p.m. at one minute intervals. Daily data analysis was conducted and also on an hourly basis where particular days within each month were analyzed in-depth. These results can be seen in the next section.

Table 5-1: Test conditions

	Number of Indoor Unit in a Cooling Mode	Number of Indoor Unit in a Heating Mode	Hot Water Demand
Test No. 1	1	6	0 Household
Test No. 2	1	6	3 Households
Test No. 3	1	6	5 Households
Test No. 4	1	6	7 Households
Test No. 5	2	5	0 Household
Test No. 6	2	5	4 Households
Test No. 7	2	5	5 Households
Test No. 8	3	4	3 Households

5.1 Performance of MFVRF System

Figure 5.1 shows the daily total energy, IUs' cooling energy, IUs' heating energy and total energy consumption with respect to the daily averaged outdoor temperature. The data shown in Figure 5.1 was obtained from the all test conditions, as shown in Table 5-1.
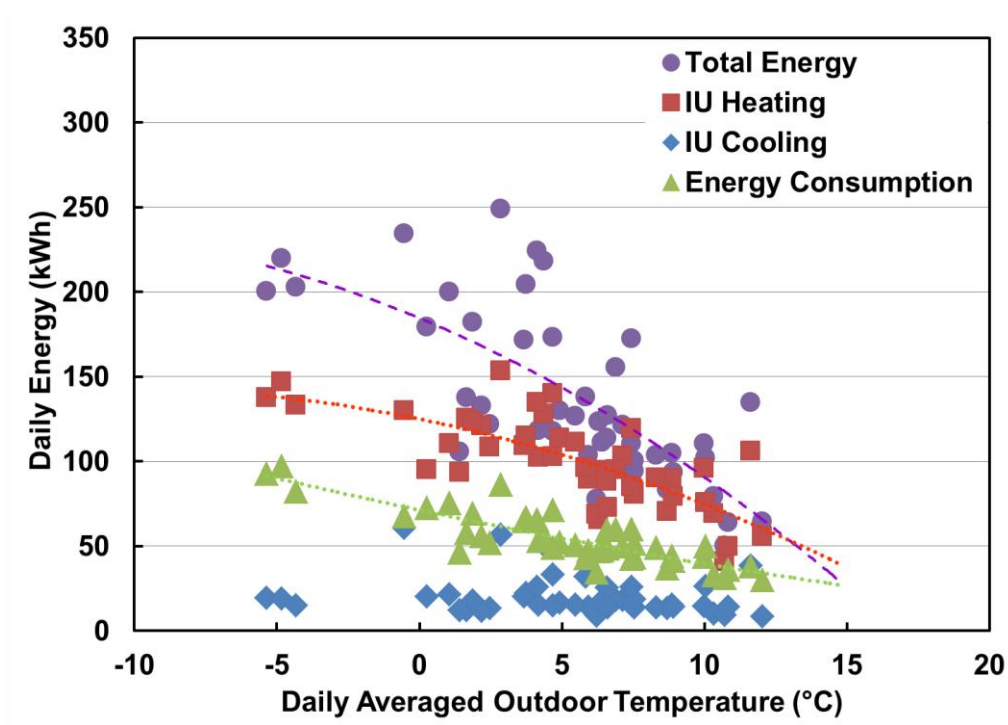
Figure 5.1: Variation of daily cooling energy, heating energy and energy consumption with respect to daily averaged outdoor temperature

Since the MFVRF system was operated in the heating-based operation mode for the test period, outdoor unit heat exchanger was used as an evaporator. As can be seen from Figure 5.1, IUs' heating energy and energy consumption were increased as the outdoor temperature was decreased as expected. Although the IUs' cooling energy was not influenced by the outdoor conditions, some data points were higher than others because of the increase in the number of cooling operated indoor unit. Higher cooling energy data points were achieved from the test No.

5 to test No. 8. Some data points about the total energy are off the trend line. This is due to the fact that the hot water demand was deliberately increased to investigate its effect, which is introduced in the next sections.
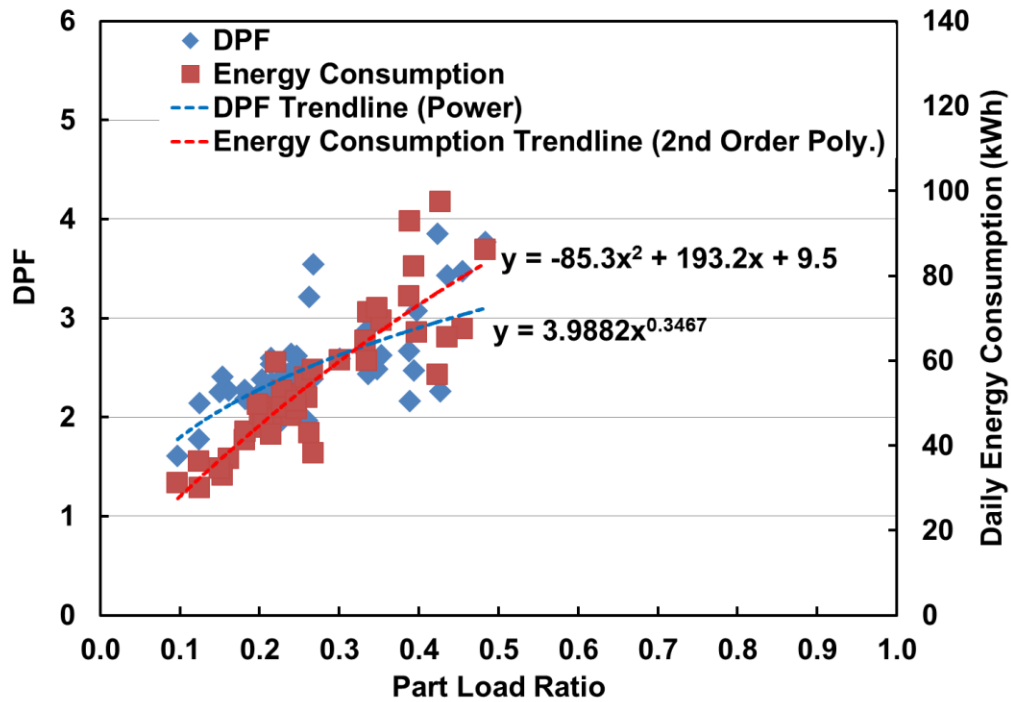
Figure 5.2: Effect of PLR on DPF and daily energy consumption

The effect of PLR on the DPF and daily energy consumption is shown in Figure 5.2. The trends of DPF and daily energy consumption are shown with power and second order polynomial trend line in Figure 5.2, respectively. As the PLR increases, the DPF and energy consumption also increased. Although the higher PLR represents more available energy than the system can produce, the DPF not always increased with PLR. This is due to the daily power consumption also increases as the PLR increases as shown in Figure 5.2.
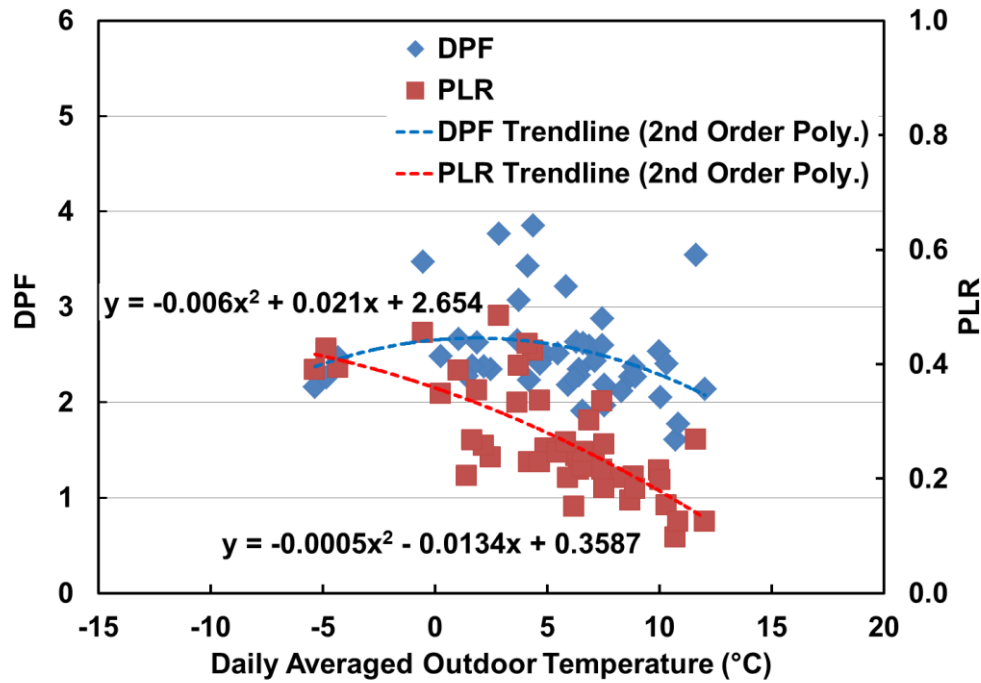
Figure 5.3: Variation of DPF and PLR with daily averaged outdoor temperature

The DPF and PLR are plotted in Figure 5.3 with respect to the daily averaged outdoor temperature during the test period. The trends are shown with second order polynomial trend line in Figure 5.3. It was observed that the PLR decreased when the daily outdoor averaged outdoor temperature increased. The low DPF at the high outdoor temperature is due to the cyclic operation of the system. The system consumes more energy than needed when the compressor starts up frequently and the room temperature is reached rapidly to the set temperature, owing to the system's oversized indoor units. It was concluded from Figure 5.3 that, even accounting for the low outdoor temperature, the daily averaged PLR was even lower than expected at 0.5. This indicates that the system installed is oversized in terms of the heating capacity. Moreover, the system consumes high energy while providing less heating capacity during each start-up.
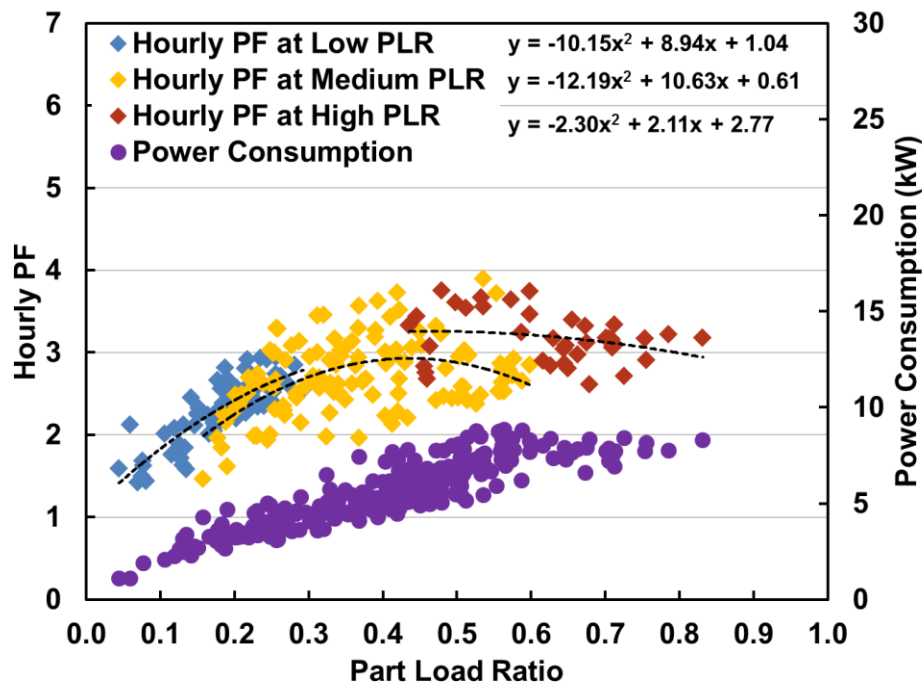
Figure 5.4: Variation of hourly performance factor and power consumption with PLR

To clearly show the effect of PLR on the system performance, the test results on particular days were analyzed on an hourly basis. Figure 5.4 shows the hourly performance factor (PF) and power consumption with the different PLR. Hourly PFs at low and medium PLR were obtained from the test No. 1 and test No. 2, 3, and 4, respectively. However, the hourly PF at high PLR cannot be achieved under the actual operating conditions, additional tests were conducted under full load conditions at night when no one occupied the office. To increase the heating load for the system, windows were fully opened and all indoor units operated at high air flow rate. Hourly PFs at high PLR are shown with red color in Figure 5.4. Variation of hourly PF with PLR presents concave distribution. Hourly PFs and power consumption at low PLR were increased as the PLR was increased. However, when the PLR is higher than 0.6, hourly PFs tended to be decreased as the PLR was increased. Hourly PFs are relatively higher when PLR is in the range of 0.5 – 0.6.

Typical coefficient of performance (COP) of electric driven heat pump is around $2.5 - 5.0$ [33]. The reason why some DPF in Figure 5.3 are lower than 2.5 is due to the oversized heating capacity of the system and cyclic operation. The capacity of the MFVRF system was decided based on the building's cooling load so that the heating capacity of the system is oversized against the heating load of the building. Moreover, the required power in the heating mode is higher than the cooling mode for the same inverter frequency [31]. Sections in the literature [31] reported that the heating performance factor of VRF system was about 2.0 over the heating season.

5.2 Effect of Hot Water Demand on the Performance of MFVRF System

In order to investigate the effect of the hot water demand on the performance of MFVRF system, the performance of the system with hot water demand was compared to that of the system without the hot water demand. Figure 5.5 shows the daily averaged water heating energy with the number of households, which was obtained from test conditions No. 2, 3 and 4, as shown in Table 5-1. The daily heating load for the MFVRF system is increased by the hot water demand. In other words, daily water heating energy increased the heating capacity, resulting in the increase in daily PLR regardless of the outdoor weather condition, as shown in Figure 5.6. However, daily PLRs at the low outdoor temperature, inside the dotted circle in Figure 5.6, show high daily PLR as compared to the other. It is because the heating load was increased by the low outdoor temperature.
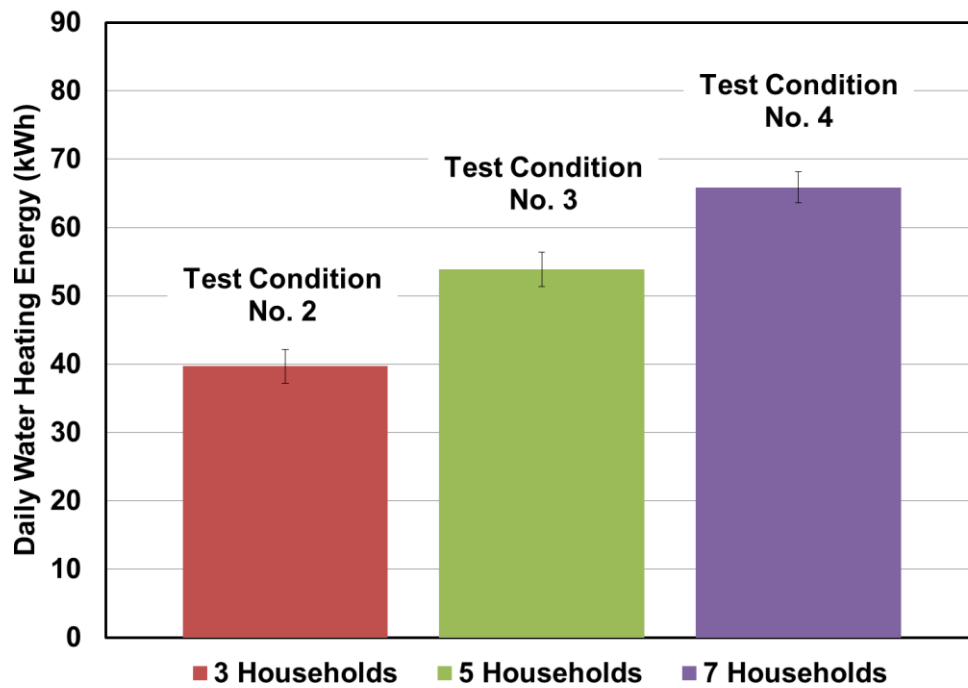
Figure 5.5: Daily water heating energy with the number of households

Figure 5.7 shows the variation of DPF with respect to PLR for a different amount of hot water demand. DPFs without hot water demand were obtained from test condition No. 1, and the DPFs with hot water demand for three, five and seven households, which were obtained from the test condition No. 2, 3 and 4, respectively. The DPFs with hot water demand were higher than that of the system operated without the hot water demand. However, some of DPFs, inside the dotted circle in Figure 5.7, shows similar DPF as compared to the DPF without hot water demand.

Figure 5.6: Daily PLR with daily averaged outdoor temperature according to the amount of hot water demand

Figure 5.7: Variation of DPF with PLR according to the amount of hot water demand

The corresponding DPFs, inside dotted circle in Figure 5.7, are shown in Figure 5.6. To clearly show the effect of hot water demand on the DPF, the DPF with respect to the outdoor temperature for each test condition is plotted in Figure 5.8. It was observed that the DPF is increased with increasing the hot water demand. When the range of the outdoor temperature is between 0 and 5 ℃, the DPF shows a tendency to increase with the hot water demand. As can be seen from Figure 5.7 and Figure 5.8, performance of the MFVRF system is highly influenced by the PLR.
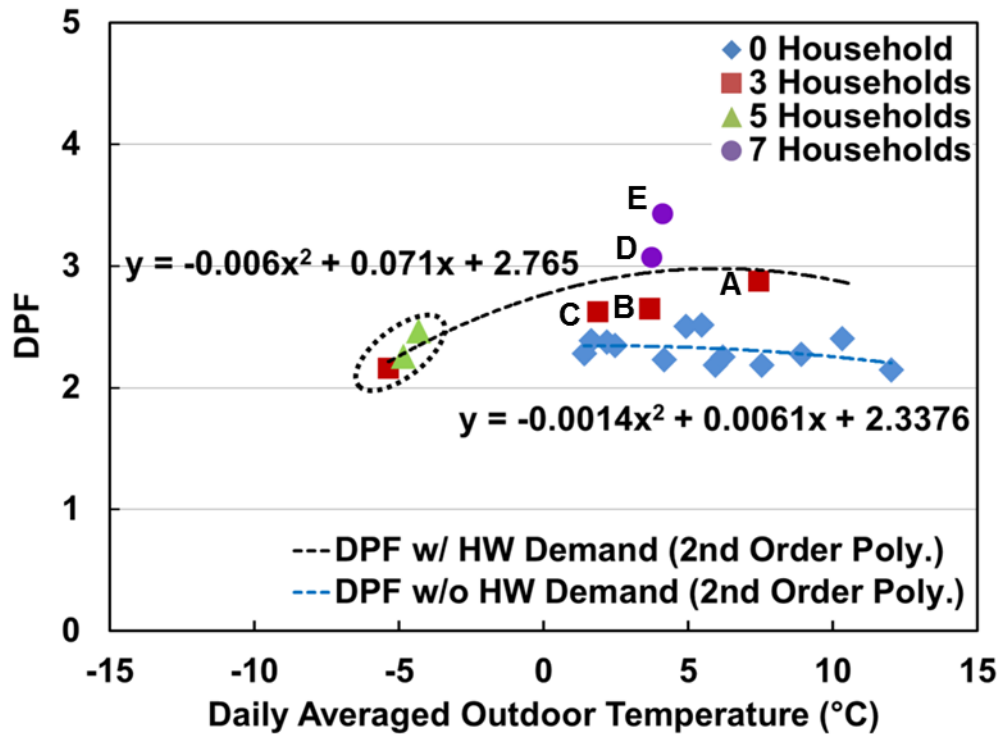
Figure 5.8: DPF with respect to daily averaged outdoor temperature according to the amount of hot water demand

Basically, performance of a typical VRF system is maximized at a certain PLR range. Due to the high internal heat gains of the office suites, the system was operated under low PLR for the

heating season. Hot water demand increases the heating load of the system, which resulted in high PLR as explained in Figure 5.6 and Figure 5.7.

Under any constant operating conditions, such as constant pressure ratio, there is an optimal frequency of the inverter-driven compressor. This action results in the highest COP, which is usually happened at the optimal frequency [34, 35]. If the compressor does not operate at optimal frequency, the inverter efficiency decreases as the difference between the operating frequency and the optimum frequency increases. Also, the outdoor unit has two compressors, fixed-speed and inverter-driven compressor. In this two-compressor system, the inverter-driven compressor always starts and ramps up first until it reaches its optimum frequency. Then, when it reaches a given pressure ratio, the fixed-speed compressor starts and the inverter-driven compressor ramps down.

Although the fixed-speed compressor is kept on to satisfy the cooling or heating load, the period of on time for the fixed-speed compressor is very short. Frequent on and off operation of the fixed-speed compressor causes high power consumption and low the heating capacity. This is due to the fact that when a compressor turns on, it requires time to reach the steady-state capacity in order to overcome thermal mass of the heat exchanger. Figure 5.9 shows the daily averaged compressor frequency with respect to daily averaged PLR according to amount of hot water demand. Error bars in Figure 5.9 represent the standard deviation of the mean value.

At a low PLR, the standard deviation of the mean compressor frequency is higher than that of compressor frequency at the higher PLR. Moreover, if the system is operating at low frequency, the system efficiency is penalized by degradation of both the compressor isentropic and

58

volumetric efficiencies. For a building with high internal heat gain in a mild climate region, the capacity of the heat pump system is typically determined based upon the cooling load. This degrades the heating performance because the system is operating under low part load condition in the heating mode. Since there exists a demand for hot water all year, the system performance can be increased by integrating the water heating system into the HR-VRF system, resulting in an improved equipment utilization rate.
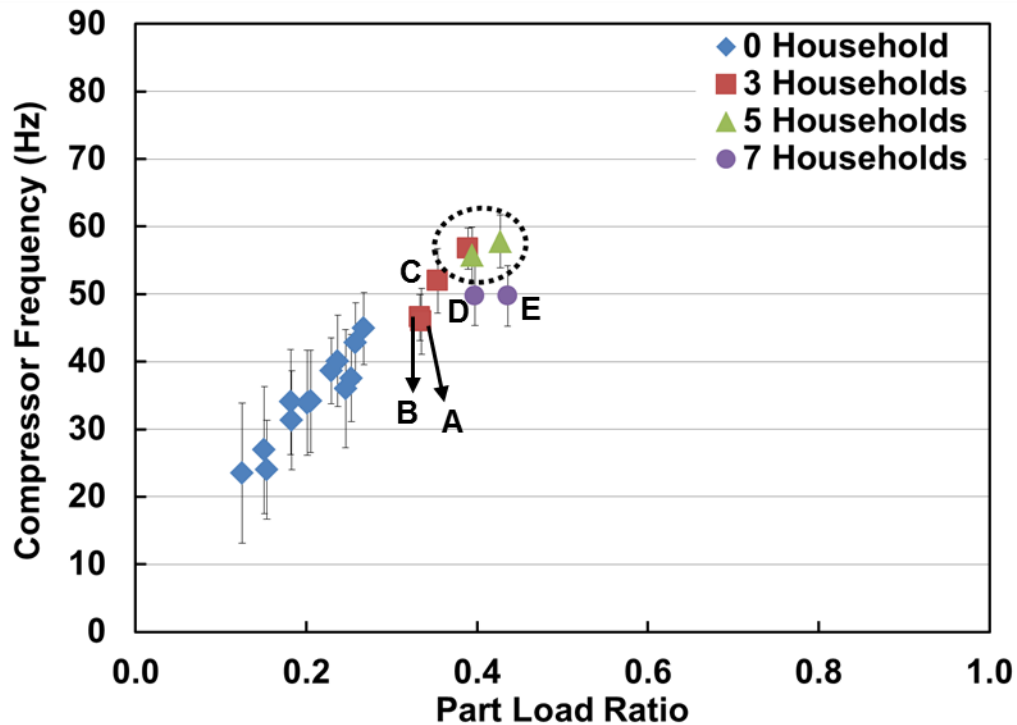
Figure 5.9: Variation of daily averaged compressor frequency with PLR according to the amount of hot water demand

5.3   Effect of Operation Mode on the Performance of MFVRF System

The effect of the operation mode on performance of the MFVRF system was investigated through the field test. For the test conditions No. 5, 6, and 7, the electric heater, which is acted as an internal heat gains, was placed in the room D to increase the cooling load. Alternatively, the

internal heat gains in the room C were high enough for the IU4 and IU5 to operate in the cooling mode. Test condition No. 8 was carried out under the actual indoor conditions. Set temperature for the cooling and heating operated indoor unit is 23 ℃.

Table 5-2: Test conditions No. 1 and No. 5 for heat recovery operation mode

	Number of Indoor Unit in a Cooling Mode	Number of Indoor Unit in a Heating Mode	Hot Water Demand
Test No. 1	1	6	0
Test No. 5	2	5	0

Table 5-2 shows the test conditions for the results shown in Figure 5.10. Figure 5.10 (a) shows the variation of DPF with the ratio of total daily cooling energy to total daily energy provided. As the ratio of total daily cooling energy to total daily energy provided was increased, DPF also increased as shown in Figure 5.10 (a). The ratio of daily total cooling energy to daily total heating energy was 13.7 and 23.2% for the test condition No.1 and the test condition No.5, respectively. At the similar daily averaged outdoor weather conditions, 5.92 and 5.87 ℃, the DPF improved about 32.2%. The DPF shown in Figure 5.10 (a) at the ratio of total daily cooling energy to total daily energy provided, 28.6% is plotted in Figure 5.10 (b).
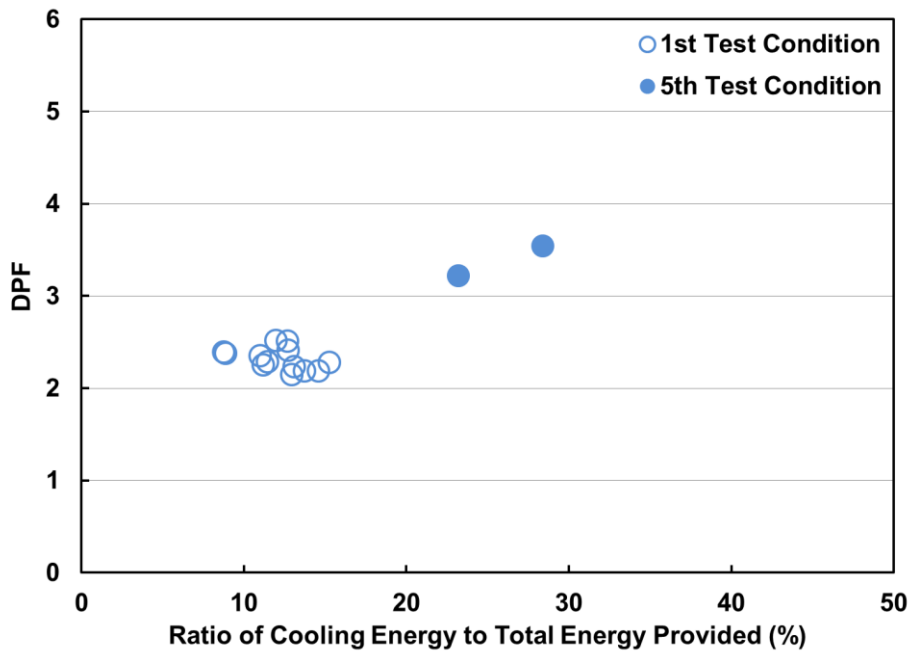
(a) Variation of DPF with the ratio of total daily cooling energy to total daily energy provided
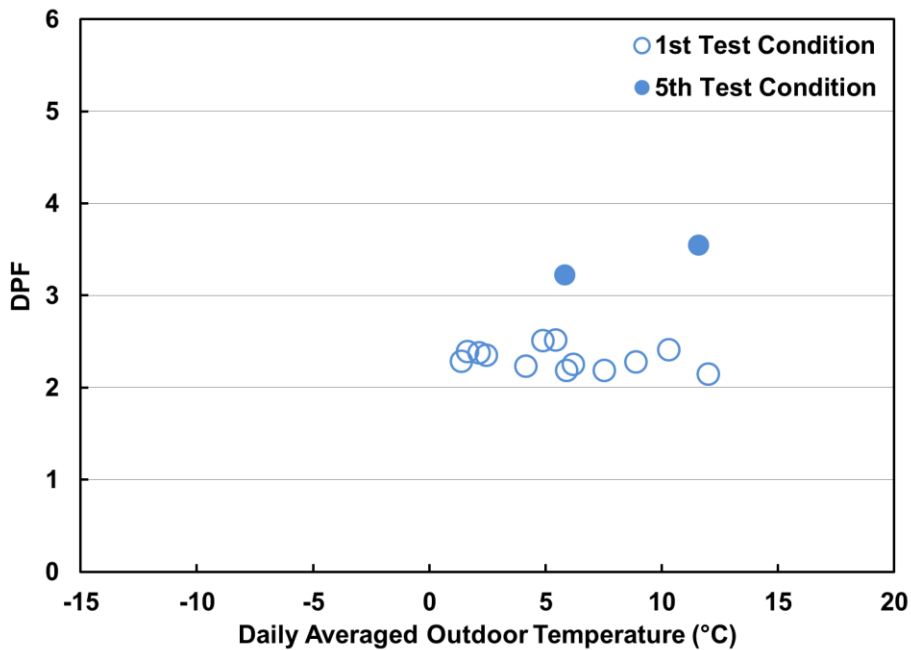
(b) Variation of DPF with respect to daily averaged outdoor temperature for different heat recovery operation mode

Figure 5.10: Effect of heat recovery operation mode on performance of MFVRF system for the 1st and 5th test conditions, (a) Variation of DPF with the ratio of total daily cooling energy to total daily energy provided, (b) Variation of DPF with respect to daily averaged outdoor temperature for different heat recovery operation mode

Figure 5.10 (b) shows the DPF with respect to daily averaged outdoor temperature. At the similar outdoor temperature about 12 ℃, DPF for the test No. 1 and test No. 5 are 2.14 and 3.54, respectively. And ratio of total daily cooling energy to total daily energy provided for the test No. 1 and test No. 5 is 13.0 and 28.4%, respectively. The DPF was improved about 39.5%.

Table 5-3: Test conditions No. 2 and No. 8 for heat recovery operation mode

	Number of Indoor Unit in a Cooling Mode	Number of Indoor Unit in a Heating Mode	Hot Water Demand
Test No. 2	1	6	3
Test No. 8	3	4	3

Additionally, test results obtained from the test conditions No. 2 and No. 8 are plotted in Figure 5.11. Table 5-3 shows the test conditions for the results. Figure 5.11 (a) shows the variation of DPF with the ratio of total daily cooling energy to total daily energy provided. As the ratio of total daily cooling energy to total daily energy provided was increased, DPF was also increased as shown in Figure 5.11 (a). The ratio of daily total cooling energy to daily total heating energy was 11.8 and 23.2% for the test condition No.2 and the test condition No.8, respectively, at the similar daily averaged outdoor weather conditions, 3.68 and 4.37 ℃. The DPF was improved about 31.2%.
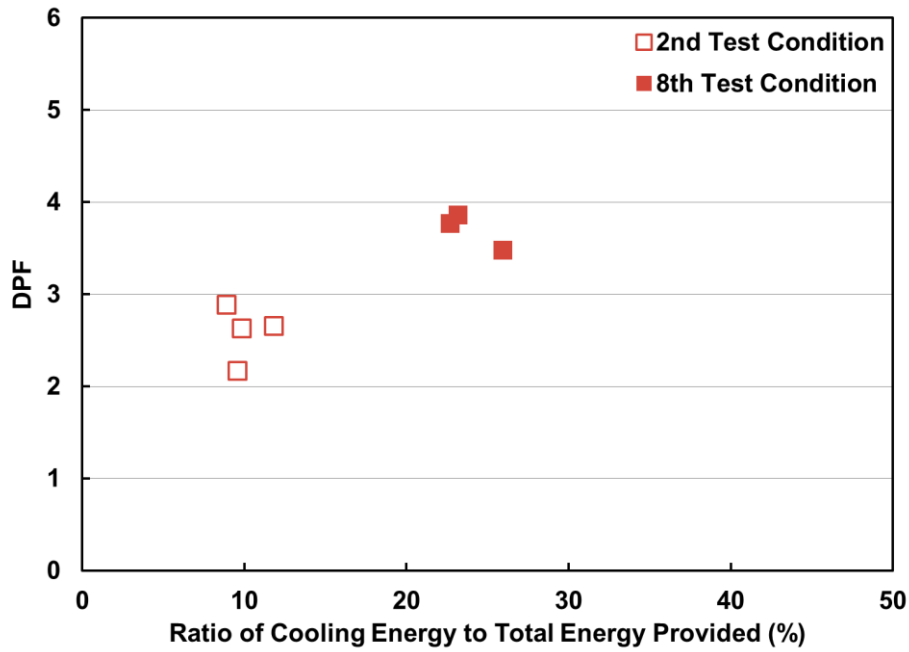
(a) Variation of DPF with the ratio of total daily cooling energy to total daily energy provided
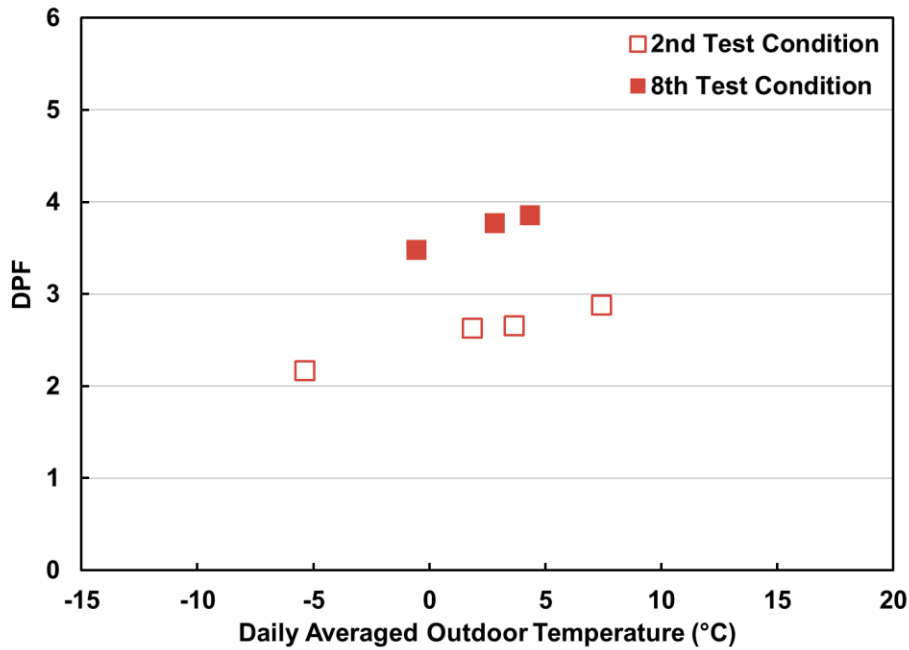
(b) Variation of DPF with respect to daily averaged outdoor temperature for different heat recovery operation mode

Figure 5.11: Effect of heat recovery operation mode on performance of MFVRF system for the 2nd and 8th test conditions, (a) Variation of DPF with the ratio of total daily cooling energy to total daily energy provided, (b) Variation of DPF with respect to daily averaged outdoor temperature for different heat recovery operation mode

In order to investigate the operating characteristics of the MFVRF system in detail in the heat recovery operation mode, an additional test was conducted under full load conditions. The ratio of sum of the cooling rated capacity of cooling operated indoor units to the sum of heating rated capacity of heating-operated indoor units was 36.5% and 5.3% for the test A and test B, respectively. Set temperatures for the cooling-operated indoor units and the heating-operated indoor units were 18 ℃ and 30 ℃, respectively. At which time, water heating system was operated continuously by consuming hot water from water tank. The tests were performed under the same compressor frequency and the same internal load when no one occupied the office. After the MFVRF system became stabilized in terms of the evaporating and condensing pressures, the data was recorded and analyzed. Figure 5.12 shows the cycle comparison in the pressure-enthalpy diagram. It was found that evaporating and condensing pressures were higher and lower, respectively, in the Test A than those in the Test B due to the decrease in the mass flow rate across the outdoor unit heat exchanger. The decreased thermal load to the outdoor unit HX leads to a decrease in evaporating pressure. Furthermore, the pressure drop across the outdoor unit heat exchanger also decreased as shown in Figure 5.12.

Table 5-4: Test result on the heat recovery operation mode

Test	Ratio of cooling to heating energy	Pressure Ratio	Total Capacity (kW)	Power Consumption (kW)	COP	Compressor Efficiency
A	36.5%	3.879	41.96	11.42	3.67	0.647
B	5.3%	4.616	31.44	12.21	2.57	0.638
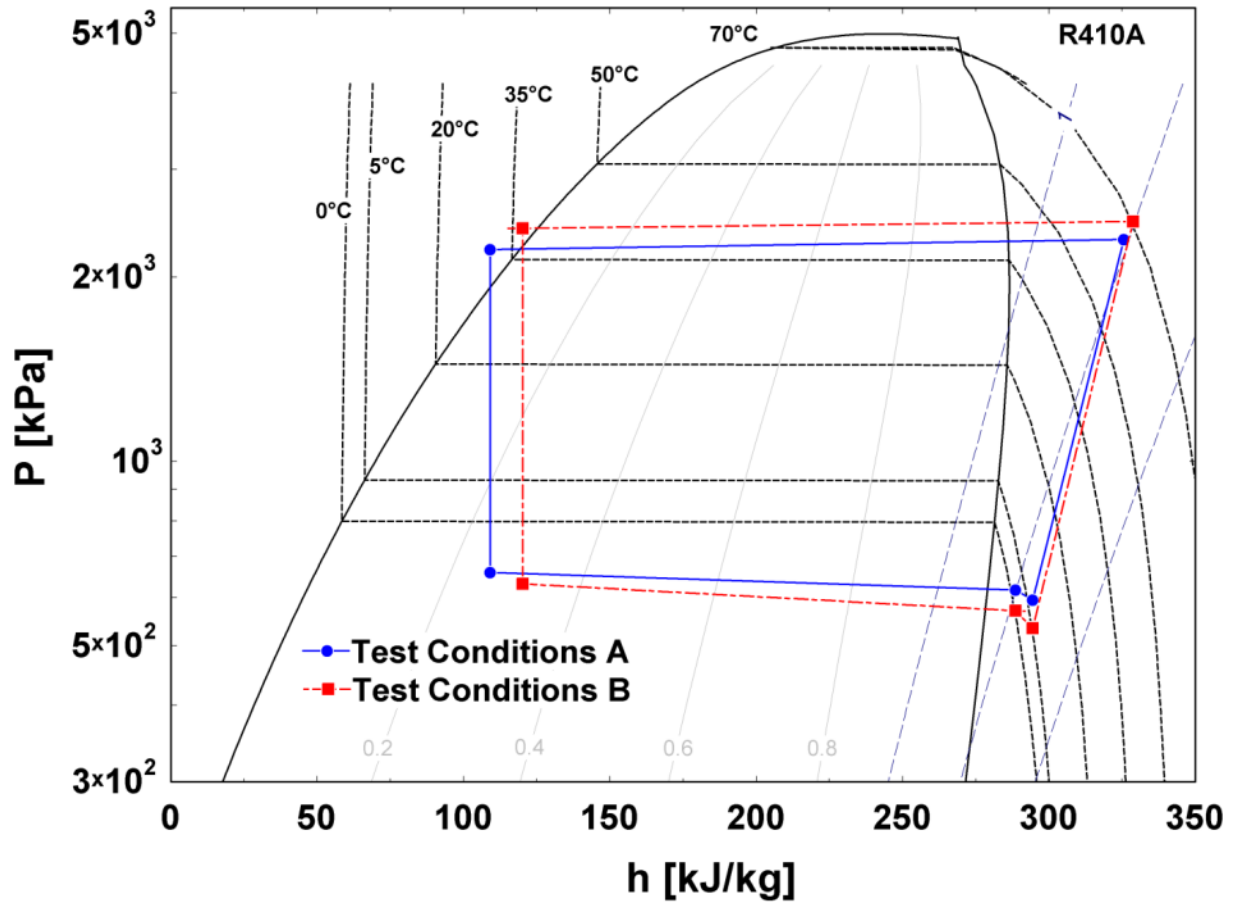
Figure 5.12: Comparison of vapor compression cycle with test A and test B in pressure and enthalpy diagram

Table 5-4 shows the summary of test result on the heat recovery operation mode. Transferring more of the recovered energy, from the indoor units operating in one mode to one or more other indoor units operating in the other mode – such as Test conditions A - increases the performance of the MFVRF system by reducing the pressure ratio of the cycle. The observation of efficiency improvements can be linked to lower thermal loads at the outdoor unit heat exchangers, which reduces the difference between vapor compression cycles condensation and evaporation temperatures.

6   Conclusions

The field performance test of the MFVRF system was carried out during a wide range of outdoor weather conditions for the heating and shoulder season. Operating characteristics of heat recovery operation mode and the benefit of the water heating system were experimentally investigated.

The MFVRF system satisfies not only the hot water demand, but provides space heating and cooling in the building. One major shortcoming for the general heat pump water heater is that its efficiency decreases as ambient temperature decreased. By integrating the water heating system into the HR-VRF system, hot water can be supplied year-round by utilizing the condensing waste heat. Typically, performance of a VRF system is maximized at a certain PLR range which is attributed to the characteristics of an inverter-driven compressor. Due to the low heating load for the building with high internal heat gain, the performance of the system decreases because of cycling losses and frequent compressor' on/off. At a low PLR, the compressor is operating at low compressor frequency, which degrades the heating performance of the system. It was found from this experiment that the DPF was improved with increase in the PLR, which resulting from the increased hot water demand.

The effect of the heat recovery operation mode on the performance of the MFVRF system was investigated through the field test. As expected, transferring the recovered energy, from the indoor units operating in one mode to one or more other indoor units operating in another mode, increased the performance of the MFVRF system. DPF was 3.54 and 2.14 when the ratio of daily total cooling energy to daily total heating energy was 28.4% and 13.0%, respectively at the

similar outdoor weather conditions, of 12 ℃. It was concluded that this is attributed to the decrease in pressure ratio and increase in the compressor efficiency.

Energy saving potential of the MFVRF system in the building with high internal heat gains, resulted in high cooling load for the summer and low heating load for the winter, and was verified through the field performance test. The performance of the MFVRF system for the heating and shoulder seasons was improved by transferring the recovered energy and the hot water supply.

7 Future Works

The field performance test of the MFVRF system was only conducted for winter and short period of shoulder seasons. Since the MFVRF system can provide space cooling, space heating and hot water simultaneously year-round, it needs to be tested for summer and whole transitional seasons. Also, experimental test result on the need to switch between cooling and heating for day and night times at the turn of the season would show the benefit of the MFVRF system.

Experimental results have to be validated against the simulation result, which will be studied with building energy simulation program, such as EnergyPro and EnergyPlus. Current available building energy simulation programs do not have a capability to model MFVRF system. Therefore, a new module which can model the MFVRF system needs to be developed.

With an experimentally validated building energy simulation program, evaluation of the performance of the MFVRF system under varying climate conditions can show the benefit of the MFVRF system for the different climate zones.

For decision makers and practitioners in the HVAC industry, they are interested in high-efficiency HVAC system in the early stage of building design. Therefore, simulation comparison of MFVRF system and other HVAC system, such as HR-VRF system with separate water heating system and HP-VRF system with additional heat pump system, would be worthy study in the future.

References

[1] DOE, available at http://buildingsdatabook.eren.doe.gov/ChapterIntro1.aspx

[2] DOE, available at http://buildingsdatabook.eren.doe.gov/TableView.aspx?table=2.1.5

[3] DOE, available at http://buildingsdatabook.eren.doe.gov/TableView.aspx?table=3.1.4

[4] ASHRAE Handbook, 2004, "HVAC Systems and Equipment: Chapter 45-Unitary air conditioners and heat pumps"

[5] Architectural Record Continuing Education Center, available at

http://continuingeducation.construction.com/crs.php?L=131&C=837

[6] Bonneville Power Administration, available at

http://www.bpa.gov/energy/n/emerging_technology/pdf/E3t_ProjectOverview_VRFOverview.pdf

[7] DOE, available at http://energy.gov/energysaver/articles/heat-pump-water-heaters

[8] Youn Cheol Park, Young Chul Kim, Man-Ki Min, "Performance analysis on a multi-type inverter air conditioner", Energy Conversion and Management, 2001, no. 42, pp 1607-1621.

[9] Fujimoto I, Takemura K., Ueno K., Saito K., Ohno K., "Performance evaluation of VRF system using refrigerant enthalpy method", ICR 2011, ID:321.

[10] Shih-Cheng Hu and Rong-Hwa Yang, "Development and testing of a multi-type air conditioner without using AC inverters", Energy Conversion and Management, 2005, no. 46, pp 373-383.

[11] Dongliang Zhang, Xu Zhang, Jun Liu, "Experimental study of performance of digital variable multiple air conditioning system under part load conditions", Energy and Buildings, 2011, no. 43, pp 1175-1178.

[12] Laeun Kwon, Yunho Hwang, Reinhard Radermacher, Byungsoon Kim, "Field performance measurements of a VRF system with sub-cooler in educational offices for the cooling season", Energy and Buildings, 2012, no. 49, pp. 300-305.

[13] Y.P Zhou, J.Y. Wu, R.Z. Wang, S. Shiochi, Y.M. Li, "Simulation and experimental validation of the variable-refrigerant-volume (VRV) air-conditioning system in EnergyPlus", Energy and Buildings, 2008, no. 40, pp 1041-1047.

[14] Yueming Li, Jingyi Wu, Sumio Shiochi, "Modeling and energy simulation of the variable refrigerant flow air conditioning system with water-cooled condenser under cooling conditions", Energy and Buildings, 2009, no. 41, pp 949-957.

[15] Laeun Kwon, Yunho Hwang, Reinhard Radermacher, Byungsoon Kim, "Modeling of Variable Refrigerant Flow System for the Cooling Season", International Refrigeration and Air Conditioning Conference at Purdue, July 2012, 2330 pp 1-8.

[16] Tolga N. Aynur, Yunho Hwang, Reinhard Radermahcer, "Simulation comparison of VAV and VRF air conditioning systems in an existing building for the cooling season", Energy and Buildings, 2009, no. 41, pp 1143-1150.

[17] Tolga N. Aynur, Yunho Hwang, Reinhard Radermacher, "The effect of the ventilation and the control mode on the performance of a VRV system in cooling and heating mode", International Refrigeration and Air Conditioning Conference at Purdue, July 2008, 2264 pp 1-8.

[18] Tolga N. Aynur, Yunho Hwang, Reinhard Radermacher, "Field performance measurements of a heat pump desiccant unit in dehumidification mode", Energy and Buildings, 2008, no. 40, pp 2141-2147.

[19] Youngju Joo, Hoon Kang, Jae Hwan Ahn, Mooyeon Lee, Yongchan Kim, "Performance characteristics of a simultaneous cooling and heating multi-heat pump at partial load conditions", International Journal of Refrigeration, 2011, no. 34, pp 893-901.

[20] Hoon Kang, Youngju Joo, Hyunjoon Chung, Yongchan Kim, Jongmin Choi, "Experimental study on the performance of a simultaneous heating and cooling multi-heat pump with the variation of operation mode", International Journal of Refrigeration, 2009, no. 32, pp 1452-1459.

[21] Yue Ming Li and Jing Yi Wu, "Energy simulation and analysis of the heat recovery variable refrigerant flow system in winter", Energy and Buildings, 2010, no. 42, pp 1093-1099.

[22] Xiaobing Liu, Tianzhen Hong, "Comparison of energy efficiency between variable refrigerant flow systems and ground source heat pump systems", Energy and Buildings, 2010, no. 42 ,pp 584-589.

[23] J.J. Guo, J.Y. Wu, R.Z. Wang, S. Li, "Experimental research and operation optimization of an air-source heat pump water heater", Applied Energy, 2011, no. 88, pp 4128-4138.

[24] Nicholas Fernandez, Yunho Hwang, Reinhard Radermacher, "Comparison of CO2 heat pump water heater performance with baseline cycle and two high COP cycles", International Journal of Refrigeration, 2010, no. 33, pp 635-644.

[25] J. Zhang, R.Z. Wang, J.Y. Wu, "System optimization and experimental research on air source heat pump water heater", Applied Thermal Engineering, 2007, no. 27, pp 1029-1035.

[26] G.L. Morrison, T.N. Anderson, M. Behnia, "Seasonal performance rating of heat pump water heaters", Solar Energy, 2004, no. 76, pp. 147-152.

[27] T.N. Anderson, G.L. Morrison, "Effect of load pattern on solar-boosted heat pump water heater performance", Solar Energy, 2007, no. 81, pp. 1386-1395.

[28] Jorn Stene, "Residential CO2 heat pump system for combined space heating and hot water heating", International Journal of Refrigeration, 2005, no. 28, pp. 1259-1265.

[29] Jie Ji, Tin-tai Chow, Gang Pei, Jun Dong, Wei He, "Domestic air-conditioner and integrated water heater for subtropical climate", Applied Thermal Engineering, 2003, no. 23, pp. 581-592.

[30] Tolga N. Aynur, "Experimental and simulation evaluation of a multi-split type air conditioning system under steady-state and transient conditions", Ph.D. Thesis, Department of Mechanical Engineering, Istanbul Technical University, Turkey, 2008.

[31] Building Energy Data Book, http://buildingsdatabook.eren.doe.gov

[32] ASHRAE Standard 90.2-2001, "Energy-Efficient Design of Low-Rise Residential Buildings".

[33] IEA Heat Pump Centre,

http://www.heatpumpcentre.org/en/aboutheatpumps/heatpumpperformance/Sidor/default.aspx.

[34] Shuangquan Shao, Wenxing Shi, Xianting Li, Huajun Chen, "Performance representation of variable-speed compressor for inverter air conditioners based on experimental data", International Journal of Refrigeration, 2004, no. 27, pp 805-815

[35] Youn Cheol Park, "Transient analysis of a variable speed rotary compressor", Energy Conversion and Management, 2010, no. 51, pp 277-287